

Pentagram Spirals

Richard Evan Schwartz *

July 19, 2013

1 Introduction

The *pentagram map* is a projectively natural map defined on the space of n -gons. The case $n = 5$ is classical; it goes back at least to Clebsch in the 19th century and perhaps even to Gauss. Motzkin [Mot] also considered this case in 1945. I introduced the general version of the pentagram map in 1991. See [Sch1]. I subsequently published two additional papers, [Sch1] and [Sch2], on the topic. Now there is a growing literature. See the discussion below.

To define the pentagram map, one starts with a polygon P and produces a new polygon $T(P)$, as shown at left in Figure 1.1 for a convex hexagon. As indicated at right, the map $P \rightarrow T^2(P)$ acts naturally on labeled polygons.

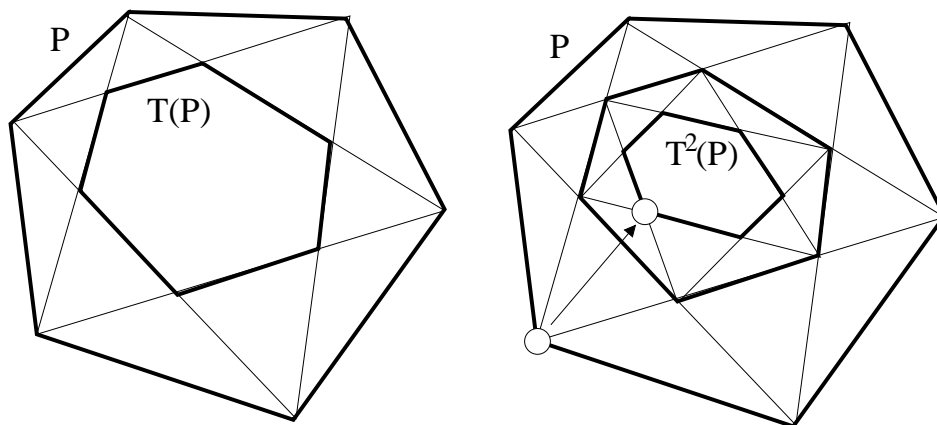


Figure 1.1: The pentagram map

*Supported by N.S.F. grant DMS-0604426

The pentagram map is defined on polygons over any field. More generally, as I will discuss below, the pentagram map is defined on the so-called twisted polygons. The pentagram map commutes with projective transformations and thereby induces a map on spaces of projective equivalence classes of polygons, both ordinary and twisted.

The purpose of this paper is to introduce a variant of the pentagram map, which I will call *pentagram spirals*. The pentagram spirals relate to the pentagram map much in the way that logarithmic spirals relate to circles. I had the idea for pentagram spirals many years ago, but since there was not much interest in the pentagram map, I decided not to pursue the idea.

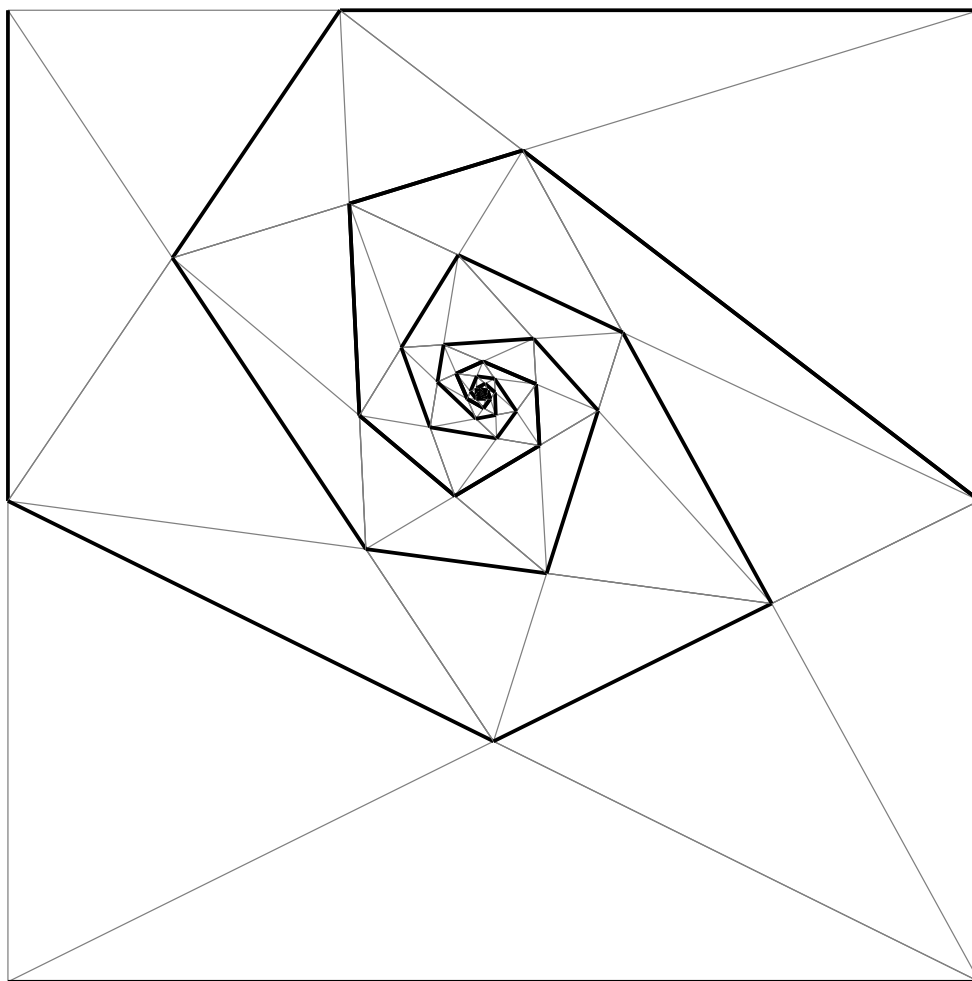


Figure 1.2: The inward half of a pentagram spiral of type $(4, 3)$.

In recent years, the pentagram map has attracted a lot of attention, thanks to the following developments.

1. In [Sch3], I found a hierarchy of integrals to the pentagram map, similar to the KdV hierarchy. I also related the pentagram map to the octahedral recurrence, and observed that the continuous limit of the pentagram map is the classical Boussinesq equation.
2. In [OST1], Ovsienko, Tabachnikov and I showed that the pentagram map is a completely integrable system when defined on the space of projective classes of twisted polygons. We also elaborated on the connection to the Boussinesq equation.
3. In [Sol] Soloviev showed that the pentagram map is completely integrable, in the algebro-geometric sense, on spaces of projective classes of real polygons and on spaces of projective classes of complex polygons. In particular Soloviev showed that the pentagram map has a Lax pair and he deduced the invariant Poisson structure from the Phong-Krichever universal formula.
4. In [OST2] (independently, at roughly the same time as [Sol]) Ovsienko, Tabachnikov and I showed that the pentagram map is a discrete, completely integrable system, in the sense of Liouville-Arnold, when defined on the space of projective classes of closed convex polygons.
5. In [Gli1], Glick identified the pentagram map with a specific cluster algebra, and found algebraic formulas for iterates of the map which are similar in spirit to those found by Robbins and Rumsey for the octahedral recurrence.
6. In [GSTV], Gekhtman, Shapiro, Tabachnikov, Vainshtein generalized the pentagram map to similar maps using longer diagonals, and defined on spaces of so-called *corrugated polygons* in higher dimensions. The work in [GSTV] generalizes Glick's cluster algebra.
7. In [MB1], Mari-Beffa defines higher dimensional generalizations of the pentagram map and relates their continuous limits to various families of integrable PDEs. See also [MB2].

8. In the recent [KS], Khesin and Soloviev obtain definitive results about higher dimensional analogues of the pentagram map, their integrability, and their connection to KdV-type equations.
9. In the preprint [FM], Fock and Marshakov relate the pentagram map to, among other things, Poisson Lie groups.
10. The preprint [KDiF] discusses many aspects of the octahedral recurrence, drawing connections to the work in [GSTV].

Though this is not directly related to the pentagram map, it seems also worth mentioning the recent paper [GK] of Goncharov and Kenyon, who study a family of cluster integrable systems. These systems are closely related to the octahedral recurrence which, in turn, is closely related to the pentagram map.

Informally, a *pentagram spiral* is a bi-infinite polygonal path P in the projective plane such that some finite power of the pentagram map carries P to itself when P is considered as an unlabeled path. §3.1 has a formal definition. The global combinatorics of how this is done allows one to describe the *type* of the spiral by a pair of integers (n, k) . For instance, k is the smallest integer such that $T^k(P) = P$, as an unlabeled path. The combinatorics of the situation will be discussed in §3.2.

For every pair (n, k) with $n \geq 4$ and $k = 1, \dots, (n - 1)$, I will introduce a *pentagram spiral* of type (n, k) . I will focus on the case when the spirals are what I call *properly locally convex*, or PLC for short. The example in Figure 1.2 is PLC. Though it is not nearly as obvious as in the case of polygons, the basic constructions which generate the polygon spirals just depend on drawing and intersecting lines in the projective plane. Thus, they make sense over essentially any field. However, we shall be interested mainly in the PLC case.

We label the vertices of the spiral by consecutive integers, so that the integers increase as the spiral moves inwards. A labeled pentagram spiral is really just the same thing as a pentagram spiral with a distinguished vertex. In §3 we will prove

Theorem 1.1 *The space $\mathcal{C}(n, k)$ of projective equivalence classes of labeled PLC pentagram spirals of type (n, k) has dimension $(2n - 8) + k$ and is diffeomorphic to an open ball.*

This result really amounts to describing how one generates pictures like Figure 1.2. The space $\mathcal{C}(n, k)$ should be seen as a relative of the space $\mathcal{C}(n)$ of projective classes of closed convex n -gons. The space $\mathcal{C}(n)$ has dimension $2n - 8$ and is diffeomorphic to an open ball.

The spaces $\mathcal{C}(n, k)$ are naturally *shift spaces*, in that there is a natural map

$$T_{n,k} : \mathcal{C}(n, k) \rightarrow \mathcal{C}(n, k) \tag{1}$$

which just amounts to moving the distinguished vertex inwards. During the course of our proof of Theorem 1.1, we will define $T_{n,k}$ from several points of view.

When properly interpreted, the map $T_{n,k}$ is a d th root of the pentagram map, where $d = 2k/(2n + k)$. At the same time, when n is large and k is small, the space $\mathcal{C}(n, k)$ is an approximation of the space $\mathcal{C}(n)$. Thus, $T_{n,k}$ in these cases is a very high root of a map which is close to the pentagram map. Independent of the intrinsic beauty of the pentagram spirals, it seems useful to have these high roots of approximations to the pentagram map.

In §4 we will introduce projectively natural coordinates on the space $\mathcal{C}(n, k)$ and exhibit a $T_{n,k}$ invariant function. This is the analog of the invariant function used in [Sch1] and [Sch2]. For experts, our first invariant function is the analogue of what is, in the closed case, one of the Casimirs for the invariant Poisson structure.

In §5 we will prove the following compactness result, which is similar in spirit to a similar result in [Sch1].

Theorem 1.2 *The orbits of $T_{n,k}$ have compact closure in $\mathcal{C}(n, k)$.*

Theorem 1.2 says that up to projective equivalence one sees roughly the same shape, over and over again, as one moves inwards or outwards along the spirals. The proof just involves showing that our invariant function has compact level sets.

In §6 we will use Theorem 1.2 to deduce several geometric corollaries about PLC pentagram spirals.

Theorem 1.3 *The ω -limit set of a PLC pentagram spiral, in the projective plane, is a union of a single point and a single line. Equivalently, the support of the triangulation associated to a pentagram spiral is projectively equivalent to a punctured Euclidean plane.*

Theorem 1.3 implies that the forward direction of P spirals down to a single *limit point*. One might wonder about the nature of this spiraling.

Theorem 1.4 *A PLC pentagram spiral winds infinitely many times around its limit point.*

Theorems 1.3 and 1.4 pin down some of the rough geometry of the triangulations associated to the pentagram spirals. Theorem 1.3 is the analog of the result in [Sch1] which says that the pentagram map shrinks arbitrary convex polygons to single points. The triangulations associated to the pentagram spirals are locally the same as the triangulations one sees when one takes the full orbit of a convex polygon under the pentagram map. However, the global structure of the tilings is different.

The main purpose of this paper is geometric. The above results answer probably the most basic geometric questions one would want to know about PLC pentagram spirals. I believe that the deep algebraic structure underlying the pentagram map is also present in the pentagram spirals, and I hope that this paper inspires future work on these objects. In the informal §7, I will discuss some computer experiments, conjectures, and topics for further study.

I wrote a Java program which allows the user to draw the pentagram spirals for smallish values of n and k , and also to watch the spirals evolve under the map $T_{n,k}$. You can download this program at

<http://www.math.brown.edu/~res/Java/SPIRAL.tar>

I strongly suggest that the reader interested in this paper download the program and play with it. I think that the program greatly enriches the paper.

This paper contains rigorous proofs of all the main results, but it seems worth mentioning that I checked the results numerically using my computer program. For instance, my program draws the pentagram spirals using exactly the formula for $T_{n,k}$ given in §3.4. The program also lets the user see that the invariant function Z defined in §4.4 is indeed an invariant of the map $T_{n,k}$.

I first thought about the pentagram spirals many years ago when I was talking to Peter Doyle about his so-called Doyle spirals. The Doyle spirals are circle packings which relate to the hexagonal circle packing much in the

way that the pentagram spirals relate to the pentagram map. Recently I walked through the streets of Nice on a pleasant spring night and thought back to the puzzles of my youth. In a nostalgic mood, I decided to send a short note about the pentagram spirals to some of the researchers interested in the pentagram map. After sending the note, I got the bug again and decided to write a more systematic paper about them.

I'd like to thank Valentin Ovsienko and Sergei Tabachnikov, my usual collaborators on the pentagram map, for many discussions about the pentagram map and related areas of mathematics. This work was carried out during my sabbatical at Oxford in 2012-13. I would especially like to thank All Souls College, Oxford, for providing a wonderful research environment. My sabbatical was funded from many sources. I would like to thank the National Science Foundation, All Souls College, the Oxford Maths Institute, the Simons Foundation, the Leverhulme Trust, the Chancellor's Professorship, and Brown University for their support during this time period.

2 Preliminaries

2.1 Projective Geometry

The *real projective plane* \mathbf{RP}^2 is the space of lines through the origin in \mathbf{R}^3 . Such lines are denoted by $[x : y : z]$. This is the line consisting of all vectors of the form (rx, ry, rz) with $r \in \mathbf{R}$.

In the usual way, we think of \mathbf{R}^2 as an affine patch of \mathbf{RP}^2 . Concretely, the inclusion is given by

$$(x, y) \rightarrow [x : y : 1]. \quad (2)$$

A *line* in \mathbf{RP}^2 is a collection of points represented by all the lines in a plane through the origin in \mathbf{R}^3 . The set $\mathbf{RP}^2 - \mathbf{R}^2$ is a single line, called the *line at infinity*. All other lines in \mathbf{RP}^2 intersect \mathbf{R}^2 in a straight line. Conversely, any straight line construction in \mathbf{R}^2 extends naturally to a straight line construction in \mathbf{RP}^2 . When we make our constructions, we will draw things in the plane (of course) but we really mean to make the constructions in the projective plane.

A *projective transformation* is a self-homeomorphism of \mathbf{RP}^2 induced by the action of an invertible linear transformation. Projective transformations permute the lines of \mathbf{RP}^2 and are in fact analytic diffeomorphisms. Conversely any homeomorphism of \mathbf{RP}^2 which carries lines to lines is a projective transformation.

A *projective construction* is one in which points and lines are produced by the following two operations:

- Given distinct points a and b , take the line (ab) through a and b .
- Given distinct lines l and m , take the intersection $l \cap m$.

We use the notation $(ab)(cd)$ to denote the intersection of the line (ab) with the line (cd) . Since projective transformations carry lines to lines, any projective construction commutes with the action of the group of projective transformations.

A subset of \mathbf{RP}^2 is *convex* if some image of that subset under a projective transformation is a convex subset of \mathbf{R}^2 in the ordinary sense. For instance, a hyperbola in the plane extends to a closed loop in \mathbf{RP}^2 which bounds a convex subset on one side. Proof: one can move the hyperbola by a projective transformation so that it is a circle in the plane.

2.2 The Cross Ratio

The *inverse cross ratio* of 4 real numbers $a, b, c, d \in \mathbf{R}$ is the quantity

$$[a, b, c, d] = \frac{(a - b)(c - d)}{(a - c)(b - d)} \quad (3)$$

When $a < b < c < d$, the quantity $[a, b, c, d]$ lies in $(0, 1)$. We will usually consider this situation.

Given 4 collinear points A, B, C, D in the projective plane, we choose some projective transformation which identifies these points with 4 numbers on the x -axis, and then we take the cross ratio of the first coordinates of these numbers. This lets us define $[A, B, C, D]$. The result is independent of any choices made. In particular

$$[A, B, C, D] = [T(A), T(B), T(C), T(D)] \quad (4)$$

for any projective transformation T .

2.3 The Corner Invariants

In [Sch3] I introduced the notion of *corner invariants* of a polygon in the projective plane. We also used these invariants in [OST1] and [OST2]. For the basic definition we will follow the notation in [OST2], but then we will revert back to an interpretation of the invariants given in [Sch3].

The *corner invariants* of a polygonal path P with successive vertices $\{v_i\}$ are defined as follows.

We define

$$x_3 = [v_0, v_1, (v_0v_1)(v_2v_3), (v_0v_1)(v_3v_4)] \quad (5)$$

$$x_4 = [v_4, v_3, (v_4v_3)(v_2v_1), (v_4v_3)(v_1v_0)]. \quad (6)$$

The remaining invariants are defined by shifting the indices by $2k$ for $k \in \mathbf{Z}$. Figure 2.1 shows a picture of the construction.

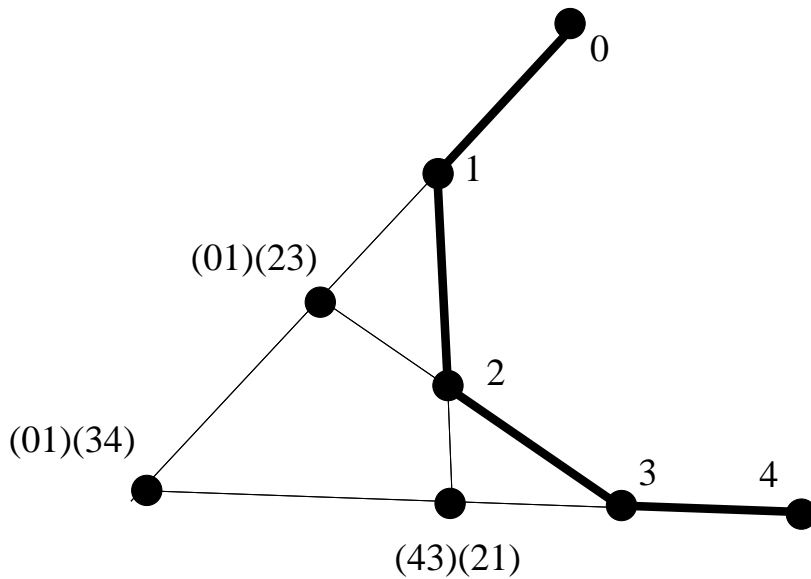


Figure 2.1: The corner invariants

When the curve is such that every 5 consecutive points make the vertices of a convex pentagon, the invariants all lie in $(0, 1)$.

The corner invariants are projectively natural. They provide projectively natural coordinates on the space of polygons. Two polygons are projective equivalent if and only if they have the same corner invariants. See [Sch3] for details. We can express the pentagram map in these coordinates, provided that we “break symmetry” and choose a less than canonical labeling scheme for P and $T(P)$. We label the vertices of $P' = T(P)$ so that

$$v'_1 = (v_0v_2)(v_1v_3). \quad (7)$$

The remaining labels are obtained by shifting the indices. In [OST2], we called this the *right convention*. Using the right convention, we have

$$x'_2 = x_4 \frac{1 - x_5x_6}{1 - x_1x_2}, \quad x'_3 = x_3 \frac{1 - x_1x_2}{1 - x_5x_6}. \quad (8)$$

The remaining equations are obtained by shifting the indices by $2k$. These equations are less than perfectly symmetric, on account of the symmetry-breaking labeling convention. However, they served our purposes in [OST1] and [OST2]. In the next section we will explain a more symmetric picture.

2.4 Tiling Interpretation of the Coordinates

For convenience we work with bi-infinite paths. Before getting to the paths, however, we will discuss a seemingly different construction. We consider a hexagonal tiling of the plane, by right-angled isosceles triangles whose hypotenuse is horizontal. Figure 2.2 shows a small part of this triangulation.

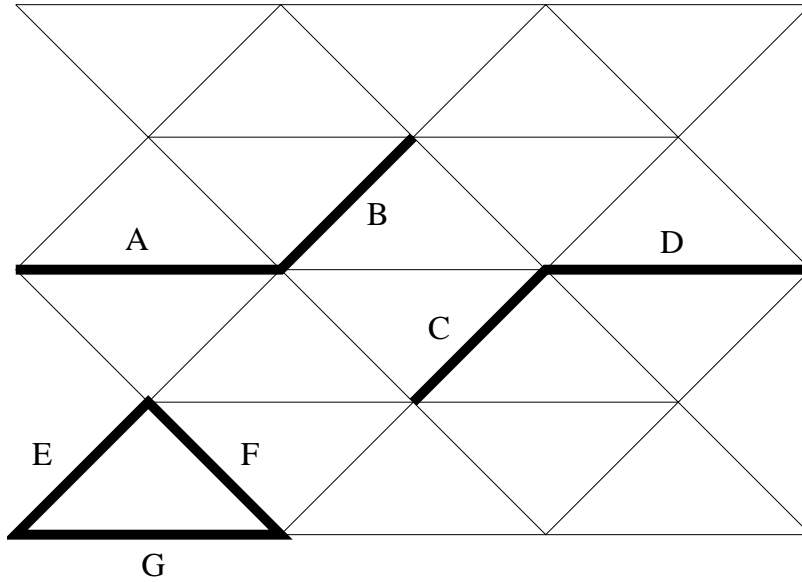


Figure 2.2: The corner invariants

We label the edges of the triangulation by real numbers and we insist on the compatibility relations

$$AB = CD, \quad G = 1 - EF. \quad (9)$$

These relations are meant to hold for the labels of all the isometric images of these configurations. The configurations may be translated or reflected. We call such a labeling a *pentagram labeling*.

If we label the diagonal edges of one row of diagonals, we can fill in the remaining labels using the compatibility rules. This will certainly remind some readers of the octahedral recurrence, and indeed we worked out the connection explicitly in [Sch3].

To see the connection between the pentagram labelings and the pentagram map, we fill in two rows of diagonal edges with the corner invariants, as in Figure 2.3.

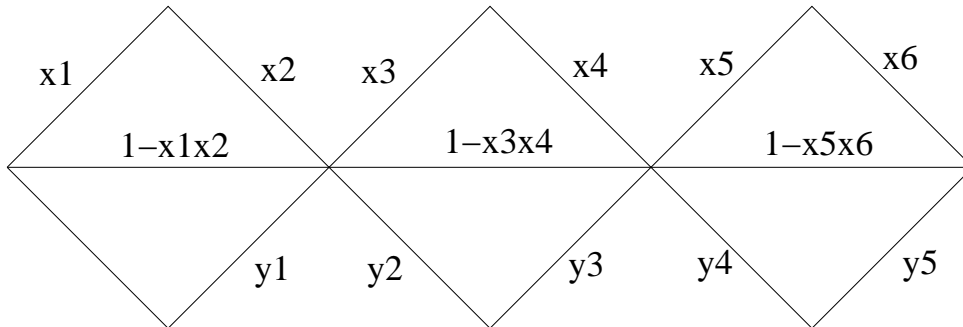


Figure 2.3: The pentagram map seen on the tiling

For ease of labeling we set $y_i = x'_i$. The compatibility rules above express the y -coordinates in terms of the x -coordinates, and the formula is exactly as given for the pentagram map in Equation 8. The cost of breaking symmetry is that the correspondence between the triangulation labels with the corner invariants is somewhat asymmetric. Indeed, if we wanted to continue this correspondence down to the next row of the tiling, so to speak, we would have to switch from the right to the left labeling convention.

In [Sch3] we used a different scheme, whereby the corner invariants corresponded not to vertices of the polygon but rather flags. The system in [Sch3] worked perfectly from the point of view of lining up the pentagram picture with the tiling picture, but the apparatus was somewhat cumbersome. Ultimately, we dropped this scheme in [OST1] and [OST2], settling on something less canonical but more businesslike. In §4 we will try for the best of both worlds, choosing a convention for the corner invariants which captures the symmetry in [Sch3] but retains the efficient nature of [OST1] and [OST2]

In case we are working in $\mathcal{C}(n)$, the labelings we get are periodic with respect to a horizontal translation by n . (We think of the horizontal edges as having unit length.) In this case, the reader can probably see that the products

$$E(P) = \prod_{i=1}^n x_{2i}, \quad O(P) = \prod_{i=1}^n x_{2i+1} \quad (10)$$

are such that

$$E(T(P)) = O(P), \quad O(T(P)) = E(P). \quad (11)$$

Thus E and O are invariants of the square of the pentagram map. These are the first invariants of many.

3 The Space of Pentagonam Spirals

3.1 Basic Definitions

It is actually not so easy to give a formal definition of a pentagram spiral. We will start out with an easy provisional definition but then we will explain the problems with it. Our final definition is somewhat more technical. In the discussion, T denotes the pentagram map, defined on unlabeled paths.

Definition: A bi-infinite polygonal path $P \subset \mathbf{RP}^2$ is a *weak pentagram spiral* if path $P \subset \mathbf{RP}^2$ with the following there is some integer $k > 0$ such that T^k is defined on P and $T^k(P) = P$. The smallest k with this property is called the *order* of P .

It is important to note that perhaps $T^k(P) = P$ only in the unlabeled sense. For instance, when k is even, there is a canonical notion of an action of T on labeled bi-infinite paths. In this situation, it might be the case that $T^k(P)$ and P do not agree as labeled paths.

The definition above is too broad to be of use to us. For example, suppose we have a polygon Q which is periodic under the pentagram map, in the literal sense that $T^k(Q) = Q$. The pentagram map has many periodic points when acting on projective classes of polygons, but here we mean that the actual polygon is periodic with respect to the pentagram map. We do not have an explicit example of this, but presumably it can happen in the non-convex case. Then we could take P to be a bi-infinite path which winds around Q infinitely often in both directions. The path Q would be a weak pentagram spiral according to the definition above.

Here is the definition we care about.

Definition: A *properly locally convex pentagram spiral* is a weak pentagram spiral P of order k such that the iterates $T^j(P)$ are embedded, locally convex, and pairwise disjoint, for $j = 0, \dots, (k - 1)$.

We will usually abbreviate *properly locally convex* to *PLC*. Figure 3.1 shows an example of a PLC pentagram spiral of order 2. These spirals are meant to go outwards as well as inwards.

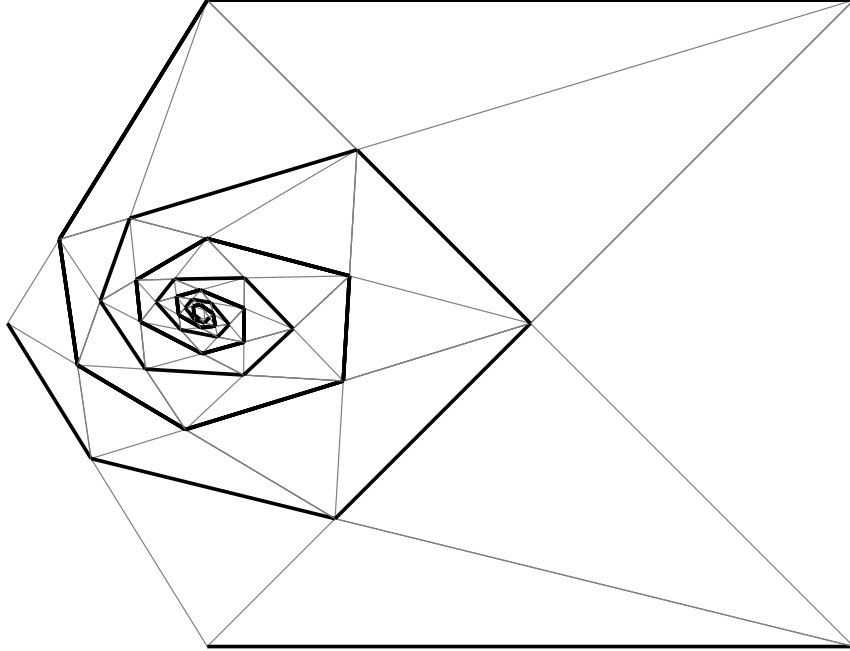


Figure 3.1: A PLC pentagram spiral of type $(5, 2)$.

We are not interested in pentagram spirals which are not PLC, but we give a formal definition for the interested reader. To make this definition go more smoothly, we will assume Theorem 1.3. Suitably normalized, a PLC pentagram spiral defines a triangulation of the punctured plane. Figure 3.1 shows the “inner half” of this triangulation. We call this tiling a PLC tiling.

Let τ denote a PLC tiling. An *adapted immersion* of τ is continuous map from τ into \mathbf{RP}^2 which maps each line segment of τ to a line segment in \mathbf{RP}^2 . We also require the map to carry each triangle of τ to a nontrivial triangle.

Definition: A *pentagram spiral* is the image of a PLC pentagram spiral under an adapted immersion of the corresponding PLC tiling.

Essentially, a pentagram spiral is an object which has the same locally combinatorial structure as a PLC pentagram spiral. Since we only discuss PLC pentagram spirals in this paper, the reader need not absorb this last definition in order to understand the rest of the paper.

3.2 Combinatorics of Pentagram Spirals

We will always work with PLC pentagram spirals, though what we say usually works for a general pentagram spiral. We label the vertices of each pentagram spiral by the integers, so that the numbers increase as one moves inwards along the spiral. In our example in Figure 3.1, the map T^2 carries P to itself but $T^2(P_j) = P_{j+6}$ for all $j \in \mathbf{Z}$. Here P_j is the j th point of P . In general, there is some number μ , either a whole or a half integer, such that

$$T^{2k}(P_j) = P_{j+2\mu k}. \quad (12)$$

The pair of numbers (μ, k) characterizes the combinatorial type of the tiling produced by iterating T on the spiral. In Figure 3.1, we have $\mu = 6$. In Figure 1.2, we have $\mu = 5\frac{1}{2}$.

We find it more convenient to replace μ with another invariant which captures the same information. We will use the pair (n, k) where k is the order of the spiral and

$$n = \mu - \frac{k}{2}. \quad (13)$$

Geometrically, it turns out that n counts the number of sides of the “seed” which generates the spiral. We will explain precisely what we mean by a seed in the next section, but informally, the seed is the outer polygon in Figures 1.2 and 3.1. So, we have $n = 4$ in Figure 1.2 and $n = 5$ in Figure 3.1.

There is a natural map on the space of pentagram spirals of type (n, k) , which we call $T_{n,k}$. The map $T_{n,k}$ shifts the labeling of a spiral by one unit. Thus $T_{n,k}(P)$ is the same unlabeled spiral as P , but the k th vertex of $T_{n,k}(P)$ is the $(k+1)$ st vertex of P . It seems at first that the map $T_{n,k}$ is trivial, but in fact, on labeled pentagram spirals we have

$$T_{n,k}^{2n+k}(P) = T^{2k}(P). \quad (14)$$

In the next several sections, we will develop the idea of generating a PLC pentagram spiral from a seed. The reason we do this is 2-fold. First, the seeds give a convenient way for drawing the spirals. Second, it turns out that $T_{n,k}$ can be interpreted as a kind of evolution operator on the set of seeds. The spirals are generated by considering the orbit of the seed under powers of $T_{n,k}$.

Once we have the basic constructions involving seeds, we will prove Theorem 1.1. The basic idea is to show that every seed generates a PCL spiral and that every PLC spiral comes from a seed. Finally, we will identify the version of $T_{n,k}$ given in terms of seeds with the shift map discussed above.

3.3 Seeds

A *seed* of type (n, k) is a strictly convex n -gon with an additional point chosen in the interior of each of the last k edges. More precisely, the vertices are points A_1, \dots, A_n and the additional B_{n-k+1}, \dots, B_n . Here B_j lies in the interior of the edge $A_j A_{j+1}$, with indices taken mod n . We will sometimes denote our seeds as (A, B) , where A is short for $\{A_1, \dots, A_n\}$ and B is short for $\{B_{n-k+1}, \dots, B_n\}$.

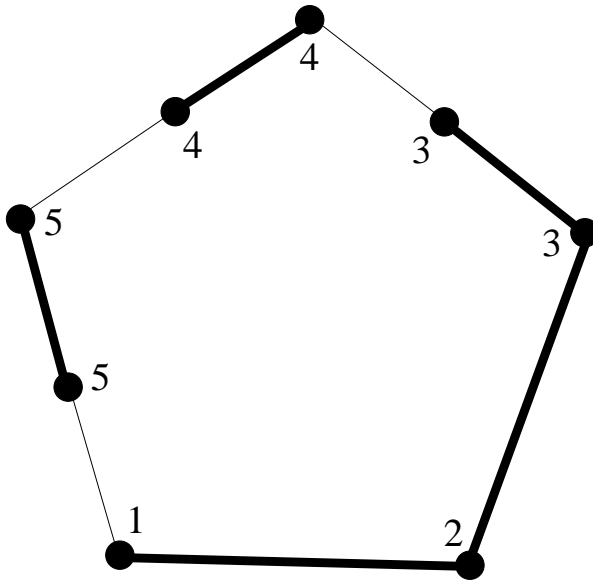


Figure 3.2: A seed of type $(5, 3)$.

Figure 3.2 shows an example of a seed of type $(5, 3)$. The labeling should be fairly obvious: The vertex labeled m denotes A_m and the point labeled m in the middle of an edge denotes B_m . We decorate the polygon with thick segments of the following kind:

- $(A_i A_{i+1})$ for $i = 1, \dots, (n - k + 1)$.
- (A_i, B_i) for $i = (n - k + 1), \dots, n$.

We call these segments the *spiral segments*. The idea is that a PLC pentagram spiral and its iterates under the pentagram map will turn out to be an infinite union of spiral segments, taken from an infinite union of seeds which piece together in a way that we explain in the next section.

3.4 The Seed Map

Figure 3.3 shows a special case of the general projective construction which produces a new seed from an old one.

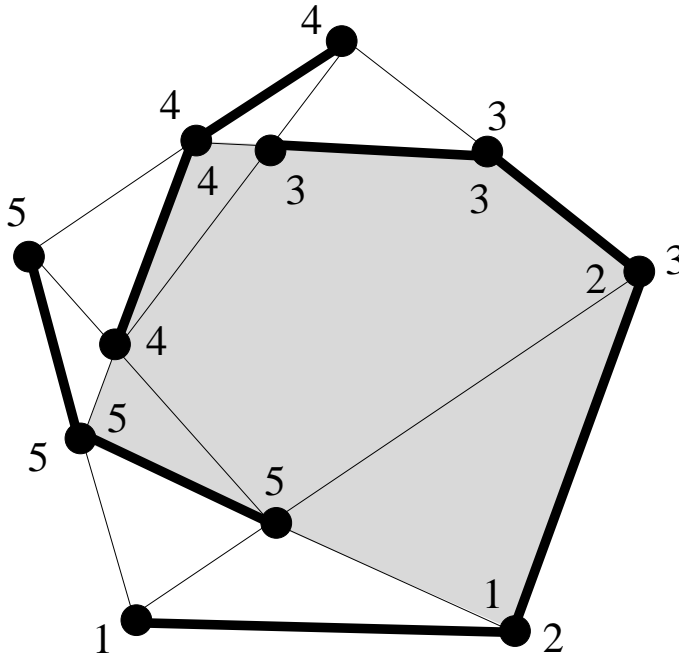


Figure 3.3: One seed produces another.

The boundary of the shaded region is the polygon supporting the new seed. The outside numbers are the old seed labels and the inside numbers are the new seed labels. Putting a star for the new points, we have

- $A_i^* = A_{i+1}$ for $i = 1, 2$.
- $A_i = B_i^*$ for $i = 3, 4, 5$.
- $B_5^* = (A_1 A_2^*)(A_5^* A_1^*)$.
- $B_i^* = (A_{i+1} B_{i+1}^*)(A_i^* A_{i+1}^*)$ for $i = 3, 4$.

In the last item, we must construct the point with the larger index ($i = 5$) first. Notice that the spiral segments on the two seeds line up to produce what promises to be a union of spirals. Figure 3.6 below adds another seed, making the connection to the pentagram map somewhat clearer.

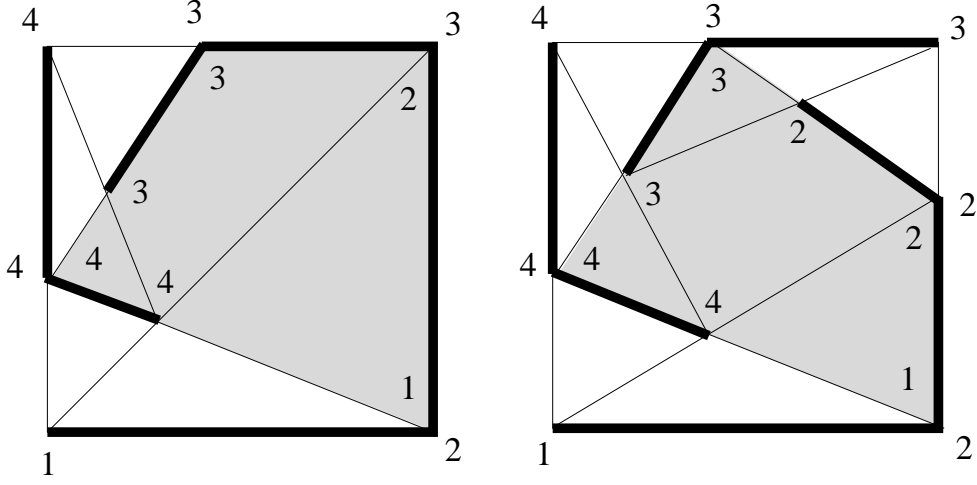


Figure 3.4: The (4, 2) and (4, 3) cases of the construction.

Figure 3.4 shows two more examples.

In general, we define

$$T_{n,k}(A_1, \dots, A_n; B_{n-k+1}, \dots, B_n) = (A_1^*, \dots, A_n^*; B_{n-k+1}^*, \dots, B_n^*) \quad (15)$$

according to the following rules.

- $A_i^* = A_{i+1}$ for $i = 1, \dots, (n - k)$.
- $A_i^* = B_i$ for $i = (n - k + 1), \dots, n$.
- $B_n^* = (A_1 A_2^*)(A_n^* A_1^*)$.
- $B_j^* = (A_{j+1} B_{j+1}^*)(A_j^* A_{j+1}^*)$ for $j = (n - 1), \dots, (n - k + 1)$.

In the last item, it is important that the points are constructed going from the largest to the smallest index, so that the map is a projective construction.

Lemma 3.1 *The starred points form a new seed of the same type.*

Proof: The A^* polygon is obtained from the A polygon by cutting off k corners using non-overlapping line segments. Hence A^* is a strictly convex polygon. The triangle $A_1 A_1^* A_n^*$ is nondegenerate and oriented counterclockwise. A routine induction argument shows that the triangles $A_j A_j^* B_j^*$ are also nondegenerate and oriented counterclockwise for $j = n, \dots, (n - k + 2)$. These facts, together with the definition of the point, imply that each B_j^* lies in the interior of the segment $A_j^* A_{j+1}^*$ ♠

3.5 The Inverse Map

Figure 3.5, which is a repeat of Figure 3.3 but with different shading, can be interpreted instead as an illustration of how one can derive outer seed from the inner one.

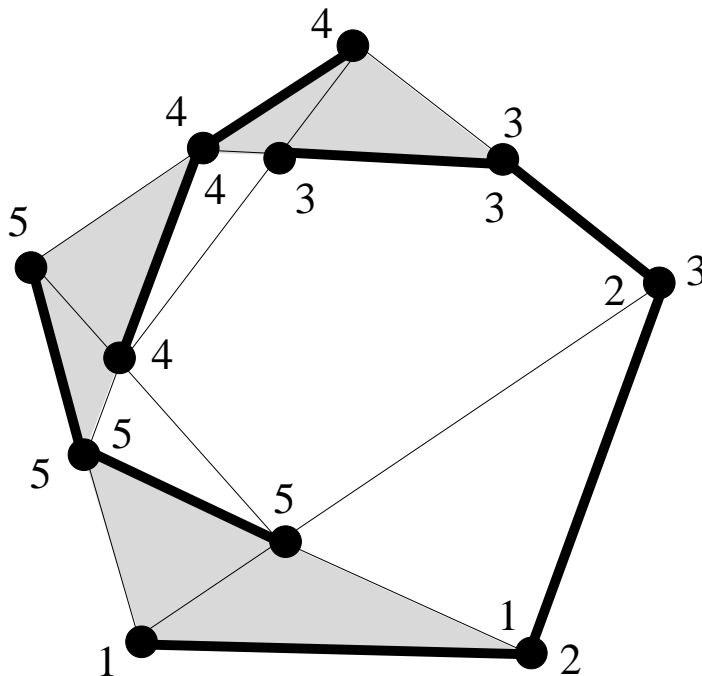


Figure 3.5: Figure 3.3 repeated.

We leave it to the reader to check that, in general,

- $A_i = A_{i-1}^*$ for $i = 2, \dots, (n - k + 1)$.
- $B_i = A_i^*$ for $i = (n - k + 1), \dots, n$.
- $A_i = (A_{i-1}B_{i-1})(B_{i-1}^*B_i^*)$ for $i = (n - k + 2), \dots, n$.
- $A_1 = (A_nB_n)(A_2^*B_n^*)$.

This gives us a formula for the inverse map $T_{n,k}^{-1}$.

It remains to check that $T_{n,k}^{-1}$ carries seeds to seeds. If we know in advance that (A, B) is a seed, then $T_{n,k}^{-1}(A^*, B^*)$ must be a seed, namely (A, B) . However, what we want to show is that $T_{n,k}^{-1}$ carries an arbitrary seed to a seed.

As readers familiar with the pentagram map know, the inverse of the pentagram map can certainly carry a convex polygon in the plane to a non-convex polygon. However, the inverse of the pentagram map always carries a convex polygon in the projective plane to a convex polygon in the projective plane. The same goes for the the seed map.

Lemma 3.2 *If (A^*, B^*) is an arbitrary seed of type (n, k) , then the pre-image $(A, B) = T_{n,k}^{-1}(A^*, B^*)$ is a seed of the same type.*

Proof: First we will show that A is a convex polygon in the projective plane. A is obtained from A^* by gluing on finitely many shaded triangles, as shown in Figure 3.5. These triangles are constructed successively, starting with $A_{n-k+1}^* A_{n-k+1}^* A_{n-k+2}$ and then going counterclockwise. A routine inductive argument shows that these triangles are never degenerate.

We know that there are some choices of seed (A^*, B^*) , namely those in the image of $T_{n,k}$, which give rise to a strictly convex polygon A . We can consider a continuous path from a seed which has this property to the seed we are interested in. The fact that the abovementioned triangles never degenerate implies that the convexity property is both an open and closed condition along our path of A -polygons. Since the initial A -polygon is strictly convex, so is the final one.

It follows from the definition of $T_{n,k}^{-1}$ that each point B_j lies on the line segment $A_j A_{j+1}$. Each edge of the form $B_j A_j$ and $B_j A_{j+1}$ appears as an edge of one of the shaded triangles. Hence these edges are all nontrivial. This forces B_j to lie in the interior of the segment $A_j A_{j+1}$. ♠

Remark: Projective dualities conjugate the pentagram map (suitably interpreted) to its inverse. The same ought to be true for the map $T_{n,k}$, provided that seeds can be interpreted in a way that puts points and lines on the same footing. The reader who stares hard enough at Figure 3.5 will eventually see that this is possible. Given the interaction with duality, the two maps $T_{n,k}$ and $T_{n,k}^{-1}$ are on the same footing and Lemma 3.2 is obvious.

It we interpret $\mathcal{C}(n, k)$ as the space of projective classes of seeds of type (n, k) , then $\mathcal{C}(n, k)$ is clearly a cell of dimension $(2n - 8) + k$. Indeed, $\mathcal{C}(n, k)$ is just a decorated version of $\mathcal{C}(n)$. The maps $T_{n,k}$ and $T_{n,k}^{-1}$ both acts as smooth diffeomorphisms on $\mathcal{C}(n, k)$. To prove Theorem 1.1, it only remains to reconcile our definition here with the ones made in §3.1.

3.6 Reconciling the Two Definitions

In this section we finish the proof of Theorem 1.1 by reconciling the two points of view, namely

1. $\mathcal{C}(n, k)$ is the space of seeds of type (n, k) and $T_{n, k}$ is the evolution operator defined above by a projective construction.
2. $\mathcal{C}(n, k)$ is the space of labeled PLC pentagram spirals of type (n, k) and $T_{n, k}$ is the shift map in this space.

Suppose we start with the first point of view. Let (A, B) be a seed. The union of the spiral segments in the bi-infinite orbit

$$\bigcup_{q \in \mathbf{Z}} T_{n, k}^q(A, B) \tag{16}$$

consists of k embedded and locally convex bi-infinite paths in the plane. To see that these paths are pentagram spirals, we just have to see that the pentagram map permutes them. This is most easily seen by looking at 3 consecutive seeds, as in Figure 3.6.

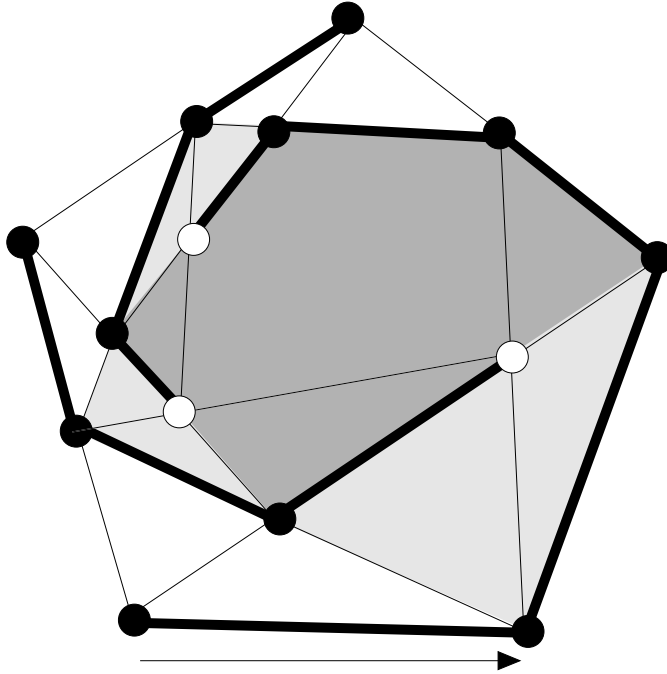


Figure 3.6: Three consecutive seeds

Looking at Figure 3.6 (and generalizing) we see that each line drawn in the construction of the *middle* seed is a shortest diagonal of one of the spirals. Since this is true for the middle seed in any sequence of 3 consecutive seeds, this fact is true for every seed in the union in Equation 16. Moreover, the white points on each spiral are revealed to be on the image of the “previous” spiral under the pentagram map. Since this is true for the corresponding points of the middle seed in every consecutive run of 3 in Equation 16, we see that the pentagram map indeed permutes the distinguished polygonal paths. Hence, these paths are all pentagram spirals.

We label our pentagram spirals so that the distinguished point is the point A_1 of the seed (A, B) . We can think of $T_{n,k}$ as acting on the union in Equation 16. $T_{n,k}$ takes this union to exactly the same union, except that it is based on the seed $(A_*, B_*) = T_{n,k}(A, B)$. All that has happened is that the new distinguished point is A_1^* , the first point of the new seed. The arrow at the bottom of Figure 3.6 points from A_1 to A_1^* . With this interpretation, $T_{n,k}$ clearly acts as the shift map on our pentagram spirals.

In short, every seed generates a labeled pentagram spiral, and the seed map acts a shift on the spiral. Thus, for at least *some* pentagram spirals, namely those generated by seeds, the two points of view coincide. It remains to see that every pentagram spiral is generated by a seed. We will be a bit sketchy in our argument because we don’t care much about the result. If it turned out that there were some exotic pentagram spirals which did not come from seeds, we would simply add the condition to our definition that the spiral come from a seed.

Lemma 3.3 *Every pentagram spiral is generated by a seed.*

Proof: Let Σ be a pentagram spiral. We interpret Σ as an infinite triangulation of some subset of the projective plane. The numbers n and k associated to Σ characterize the global combinatorics of the tiling. Let Σ' be a pentagram spiral produced by a seed of type (n, k) . The tiling Σ' has the same combinatorics as the tiling Σ . That is, there is a homeomorphism h which carries the one triangulation to the other – vertices are taken to vertices and edges are taken to edges. Moreover, certain triples of edges in Σ and in Σ' line up to form longer line segments – the diagonals used in the pentagram map. h respects this additional collinearity. Evidently h maps a seed for Σ' to a seed for Σ . ♠

4 Invariant Coordinates

4.1 Flags

We mentioned in §2.4 that we would improve upon the labeling scheme from §2. The key is to use flags rather than points or lines. On a polygonal path, a *flag* is a pair (v, e) where v is a vertex of the path and e is an edge of the path. We indicate the flag (v, e) with an auxiliary point placed on the edge e two-thirds of the way towards v . Figure 4.1 shows what we mean.

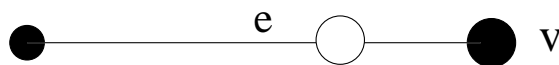


Figure 4.1: Denoting the flag (v, e) .

Suppose we have an oriented polygonal path, as shown in Figure 4.2. We orient the flags according to the following scheme.

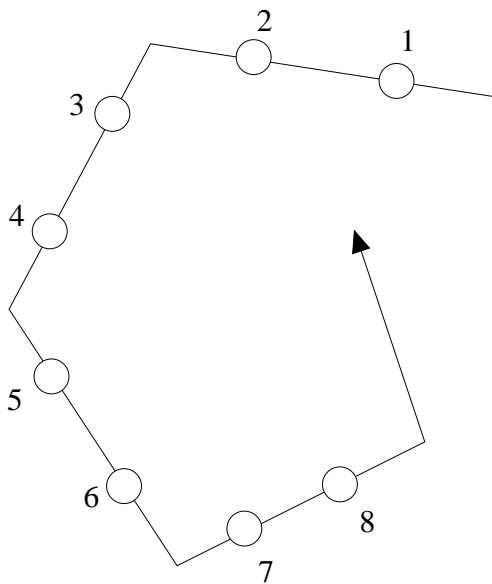


Figure 4.2: Ordering the flags along an oriented path

Finally, to each flag along such a path, we associate the cross ratio of the associated points shown in Figure 4.3. This picture is meant to be invariant under projective transformations. We call these the *flag invariants*.

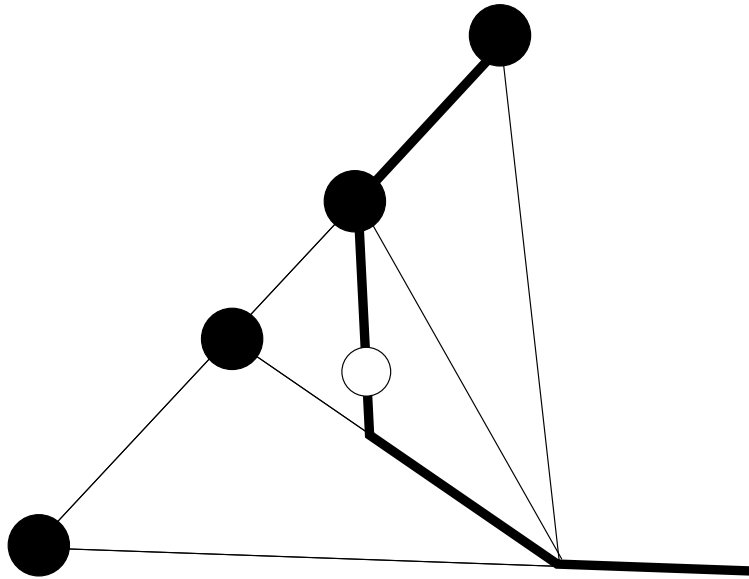


Figure 4.3: Invariant of a flag

Let us consider the naturality of this construction. The cross ratio of interest can be computed in two ways. First of all, it is the cross ratio of the 4 points shown. Two of the points involved are adjacent to the flag point. On the other hand, the cross ratio can be computed as the cross ratio of the 4 drawn lines. Two of the lines are adjacent to the line of the flag, going in the other direction from the abovementioned points. Indeed, the entire picture is invariant not just under projective transformations but also projective dualities. Were we to apply a projective duality to the picture, producing another polygonal curve (with points and lines interchanged) the invariant associated to the flag would be the same. In short, the invariant we have associated to the given flag is the canonical choice.

Moreover, the ordering of the flags in Figure 4.2 reproduces the ordering of the invariants listed in §2.3. The difference is that, when we work with the flags, there is a canonical way to line up the variables of the path P and its image $T(P)$ under the pentagram map. Figure 4.4 below shows this. With this new scheme, there is a natural way to transfer the flag labels to the hexagonal tiling so that the compatibility conditions hold. The method is such that same-numbered flags correspond to diagonal edges whose centers are on the same vertical. This is illustrated in Figure 4.5. With this new scheme, one need not change labeling conventions at each level.

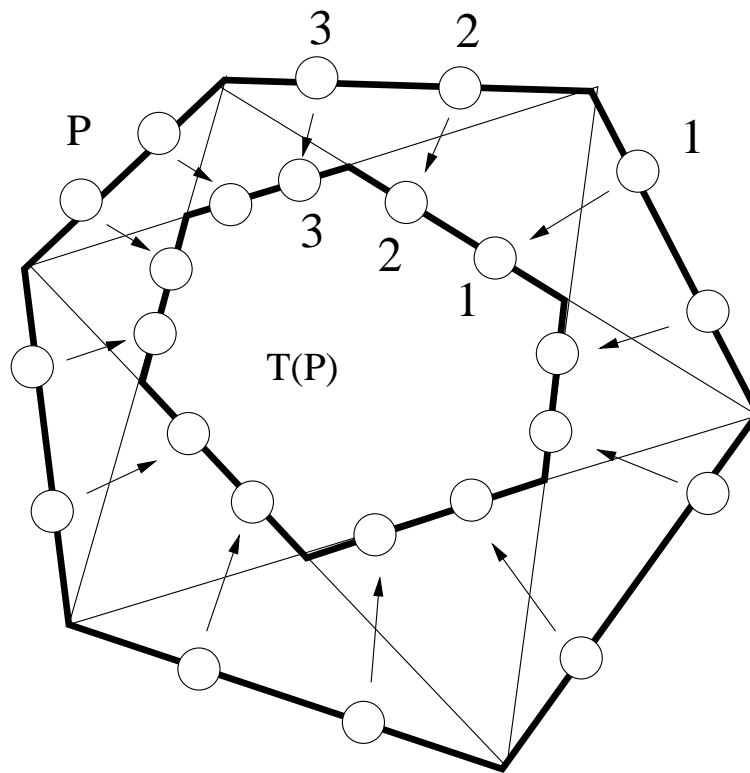


Figure 4.4: Canonical labeling for the pentagram map.

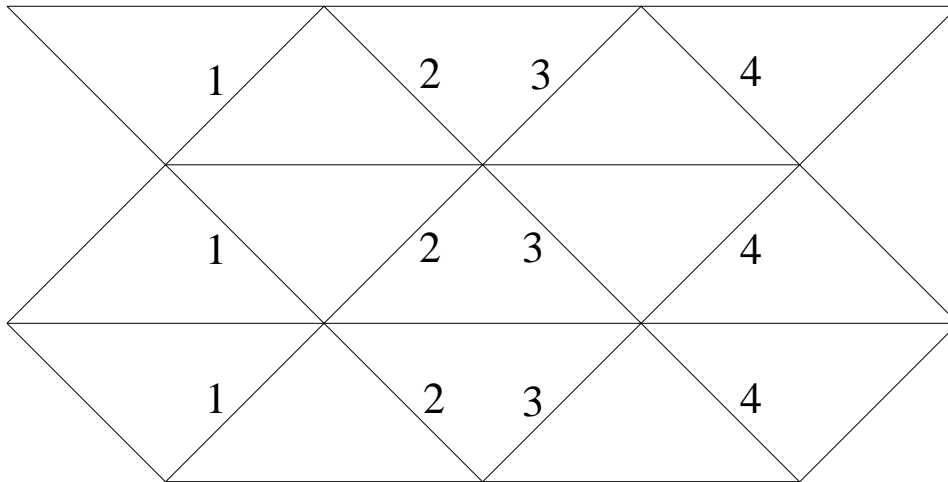


Figure 4.5: Transfer of labels to the tiling.

4.2 Pentagram Tilings Revisited

Let \mathbf{T} denote the infinite triangular tiling discussed in §2.4. Again, we normalize \mathbf{T} so that the horizontal edges have length 1. The height of each triangle is $1/2$. Let \mathcal{T} denote the set of all pentagram tilings of the edges of \mathbf{T} .

Let $\mathcal{T}(n, k)$ denote the set of pentagram tilings which are invariant under translation by the vector

$$V_{n, k} = \left(n + \frac{k}{2}, \frac{k}{2}\right). \quad (17)$$

This vector has half-integer coordinates, and the sum of the two coordinates is an integer. Hence, translation by $V_{n, k}$ is an isometry of \mathbf{T} . Thus, the definition of $\mathcal{T}(n, k)$ is not vacuous.

Comparing the discussion in §3.1 with the scheme for transferring the flag invariants of flags to the labels of \mathbf{T} , we see that each element of $\mathcal{C}(n, k)$ gives rise to a unique element of $\mathcal{T}(n, k)$. To make this completely precise, we translate \mathbf{T} so that one vertex lies at the origin. We arrange that the diagonal edge joining $(0, 0)$ to $(1/2, 1/2)$ (respectively to $(-1/2, -1/2)$) corresponds to the flag just inward (respectively outward) from the distinguished vertex of the spiral. Thus, when we move righward along horizontal edges, it corresponds to going inward along the spiral. When we move downward, it corresponds to doing the pentagram map.

It is not true that every element of $\mathcal{T}(n, k)$ arises from an element of $\mathcal{C}(n, k)$. For one thing, all the labels would have to lie in $(0, 1)$. See §5.1. For another thing, the dimensions of the spaces do not match up. For instance, in the toy case when $k = 0$, the former space has dimension $2n$ and the latter space has dimension $2n - 8$. The other elements in $\mathcal{T}(n, 0)$ correspond to the so-called *twisted polygons*. In §7 we will informally discuss a similar interpretation of the general element of $\mathcal{T}(n, k)$. Here we will only consider elements of $\mathcal{T}(n, k)$ which come from elements of $\mathcal{C}(n, k)$.

Remark: The elements of $\mathcal{T}(n, k)$ can be considered as edge labelings of a triangulation of the cylinder $\mathbf{R}^2/V_{n, k}$. The combinatorics of this triangulation is essentially the same as the combinatorics of the tiling obtained from the pentagram spiral, though the edges of the one triangulation do not precisely match up with the edges of the other. We leave it to the interested reader to work out the exact correspondence.

4.3 Discussion of Formulas

It might be nice, or at least useful for further research, to give explicit formulas for the action of $T_{n,k}$ on $\mathcal{C}(n, k)$. This amounts to identifying $\mathcal{C}(n, k)$ with a specific algebraic variety, and then expressing $T_{n,k}$ as a birational transformation of that variety. Essentially all the papers on the pentagram map take this approach.

We have seen above that each element of $\mathcal{C}(n, k)$ gives rise to an edge-labeling of a triangulation of $\mathbf{R}^2/V_{n,k}$. The labeling satisfies the above compatibility rules, and there is some finite list \mathcal{L} of edges such that the labels on \mathcal{L} determine all the other labels. Thus, one can realize $\mathcal{C}(n, k)$ as an algebraic variety in a finite dimensional space. Using the compatibility rules, one can express $T_{n,k}$ as a birational map.

For the pentagram map, this approach is completely successful. There is a canonical choice for \mathcal{L} , and the compatibility rules give rise to a transformation with a very nice formula. See [Sch3], [OST1], and [OST2]. However, for the pentagram spirals, I have not been able to find a good choice for \mathcal{L} . No choice seems canonical, and all choices seem to lead to messy formulas.

This state of affairs does not (yet) bother me. I think that the right point of view is that elements of $\mathcal{C}(n, k)$ are simply these labeled triangulations with the compatibility rules and the map $T_{n,k}$ is just a shift operator on the space of such labelings. However, I can see that this answer will be unsatisfying to some readers, and perhaps I will eventually find it unsatisfying. I hope with the interested reader will take up the question of finding good formulas in the sense discussed above. This main point of the discussion is that the problem is nontrivial.

4.4 The First Invariant

We will use a pictorial method for representing polynomial invariants of the map $T_{n,k}$. Let C be some collection of edges of \mathbf{T} . The product of the labels of the variables associated to the edges constituting C is a monomial which we denote by $\langle C \rangle$. So, $\langle C \rangle$ denotes a function on $\mathcal{T}(n, k)$ defined by C .

Given a vector V , we say that $\langle C \rangle$ is *V-invariant* if the two functions $\langle C \rangle$ and $\langle C + V \rangle$ agree on $\mathcal{T}(n, k)$. Here $C + V$ is the copy of C which has been translated by V . This definition only makes sense when translation by V preserves \mathbf{T} . We call such vectors *allowable*. Though n and k are not explicitly mentioned, it is understood that the notion of invariants is defined

with respect to these parameters.

Figure 4.5 shows the configuration C associated to the pair $(n, k) = (4, 3)$. This configuration “goes up” $4 + 3 = 7$ steps and then ”does down” 4 steps. Translation by $V_{4,3}$ identifies the endpoints of C and thus C defines a closed path on the cylinder $\mathbf{R}^2/V_{4,3}$ discussed in the remark at the end of the last section. We will use the notation $Z(4, 3)$ to denote the corresponding function $\langle C \rangle$ in this case. The general definition of $Z(n, k)$ follows the same pattern.

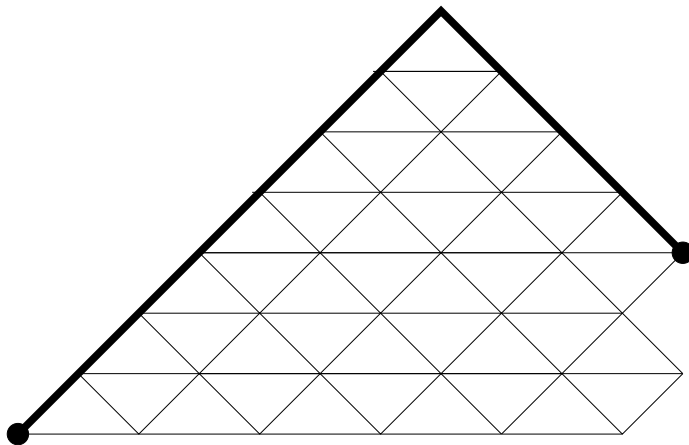


Figure 4.5: The monomial $Z(4, 3)$.

Below we will prove that $Z(n, k)$ is invariant with respect to any vector of \mathbf{T} . Before we prove this result, we need to make a short digression. Say that a *zigzag* is a path which moves rightward, along diagonal edges of \mathbf{T} and joins two vertices of \mathbf{T} .

Lemma 4.1 *Suppose that Z_1 and Z_2 are zigzags which start and end at the same vertex. Then $\langle Z_1 \rangle = \langle Z_2 \rangle$.*

Proof: If we push a zigzag across a single square, as shown in Figure 4.6 below, the corresponding monomial does not change, thanks to the pentagram relations. So, we just keep pushing the one zig-zag until it equals the other. ♠

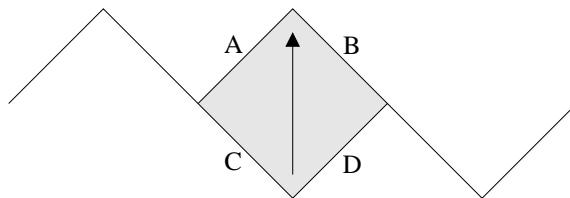


Figure 4.6: pushing a zigzag: $AB = CD$.

Lemma 4.2 $Z(n, k)$ is invariant with respect to the vector $(1, 0)$.

Proof: Let C be such that $Z(n, k) = \langle C \rangle$ and let $C' = C + (1, 0)$. Let $Z'(n, k) = \langle C' \rangle$. Referring to Figure 4.7, we have

$$C = A \cup B; \quad C' = A' \cup B'. \quad (18)$$

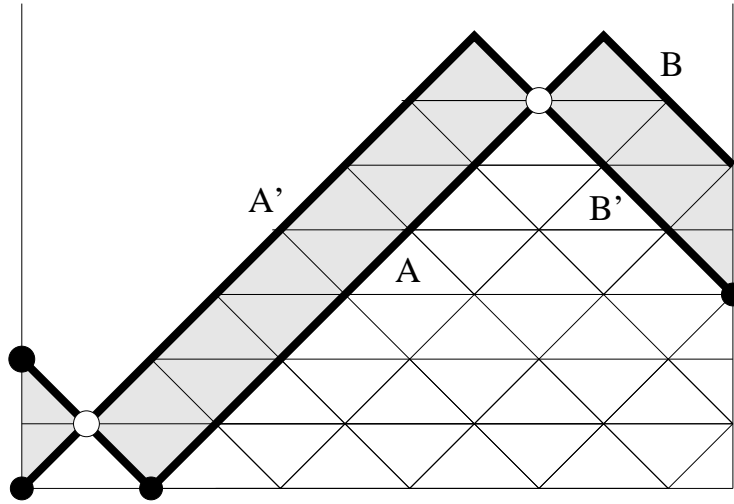


Figure 4.7: $C \cup C'$ drawn on the cylinder $\mathbf{R}^2/V_{4,3}$.

By the lemma, we have $\langle A \rangle = \langle A' \rangle$ and $\langle B \rangle = \langle B' \rangle$. Finally, we have $Z(n, k) = \langle A \rangle \langle B \rangle$ and $Z'(n, k) = \langle A' \rangle \langle B' \rangle$. ♠

Essentially the same argument works for the vector $(1/2, 1/2)$. Since the vectors $(1, 0)$ and $(1/2, 1/2)$ generate \mathbf{T} , we see that $Z(n, k)$ is invariant with respect to any allowable V .

5 Compactness of the Orbit Closures

5.1 Local Convexity

Our main goal in this chapter is to prove Theorem 1.2. For ease of exposition we will assume that $(n, k) \neq (4, 1)$. Theorem 7.1 from the next chapter takes care of this exceptional case.

Lemma 5.1 *Let P be a PLC pentagram spiral whose type is not $(4, 1)$. Every 5 consecutive points of P are the vertices of a strictly convex pentagon.*

Proof: Let (n, k) be the type of P . It suffices to consider the points P_1, P_2, P_3, P_4, P_5 and let (A, B) be the seed such that $A_1 = P_1$ and $A_2 = P_2$. There are several cases.

If $n - k \geq 4$, then $P_i = A_i$ for all i , and the result is clear: A is a strictly convex polygon.

If $n - k = 3$ (and $n > 4$) then $P_i = A_i$ for $i = 1, 2, 3, 4$ and $P_5 = B_4$. Again, by construction, the result is true.

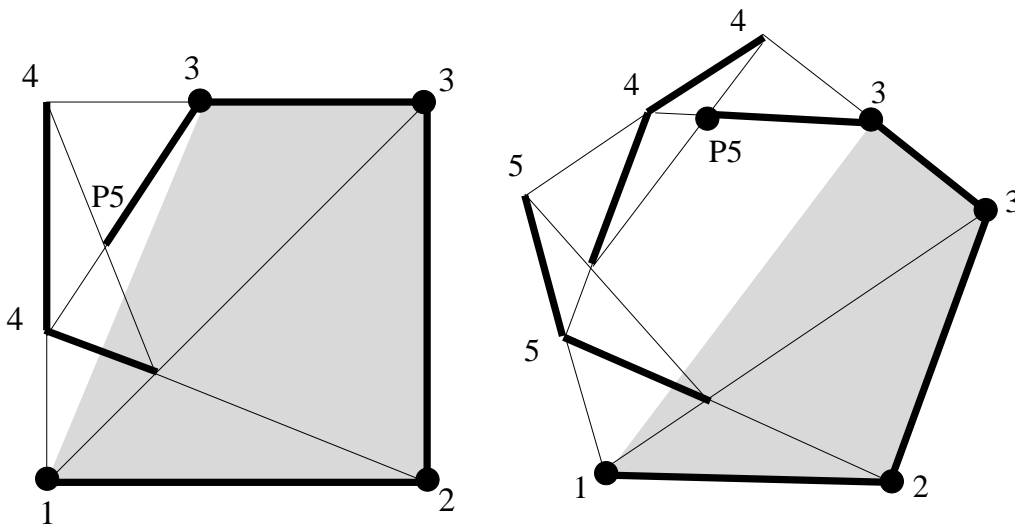


Figure 5.1: The case when $n - k = 2$ for $n = 4, 5$.

If $n - k = 2$ then $P_i = A_i$ for $i = 1, 2, 3$ and $P_4 = B_3$. The points P_1, P_2, P_3, P_4 therefore form the vertices of a convex quadrilateral Q , shaded in Figure 5.1. The line P_4P_5 , which coincides with the line B_3B_4 , lies outside Q and inside the convex polygon bounded by A . These two properties imply our result.

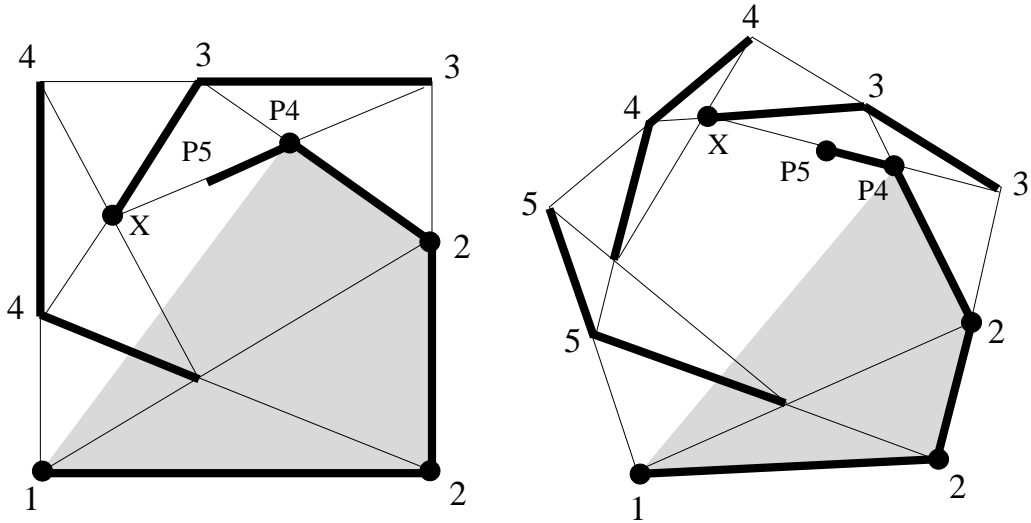


Figure 5.2: The case when $n - k = 1$ for $n = 4, 5$.

If $n - k = 1$ then $P_i = A_i$ for $i = 1, 2$ and $P_3 = B_2$. The same argument as in the preceding section shows that P_1, P_2, P_3, P_4 form the vertices of a convex quadrilateral Q , shaded in Figure 5.2. The segment B_3B_4 , which contains the point marked X , lies outside Q . Hence X lies outside Q as well. But then P_5 , which lies on the line segment P_4X , lies outside Q as well. Finally, the segment P_4A lies inside the convex polygon bounded by A . These properties imply the result. ♠

Given a pentagram spiral P of type (n, k) , let $Z(P)$ denote the value of the invariant $Z(n, k)$ evaluated on P .

Corollary 5.2 *Suppose that P is a PLC pentagram spiral. The flag invariants associated to P all lie in $(0, 1)$. Hence $Z(P)$ serves as a lower bound for the flag invariants.*

Proof: Each flag invariant is computed using 5 points, as in Figure 4.3. The convexity of the 5 points guarantees that the 4 points relevant for the cross ratio come in order along the line. Hence, all the flag invariants lie in $(0, 1)$. Given the invariance of $Z(n, k)$ with respect to any allowable vector, as established in §4.4, we see that $Z(P)$ can be computed as a product of flag invariants, one of which is the one that currently interests us. ♠

5.2 The Vertex Invariant

In this section we associate a different invariant to the the vertices (as opposed to the flags) of a locally convex polygonal path.

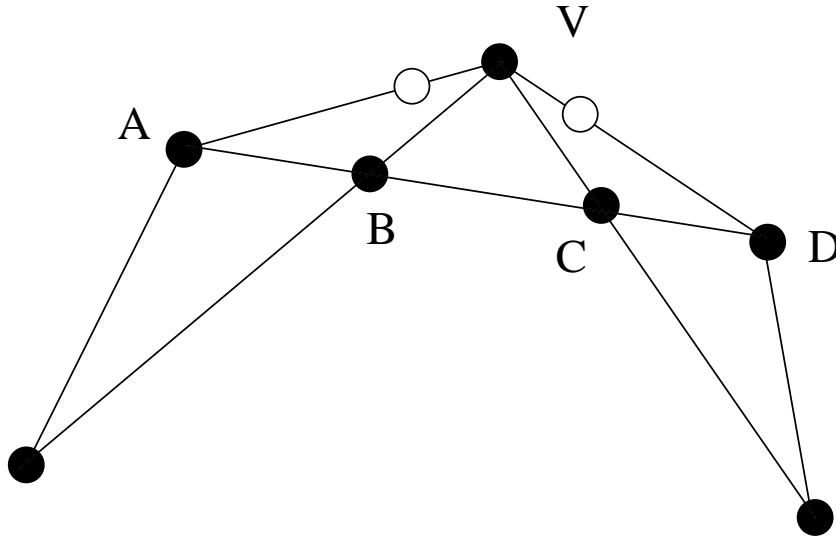


Figure 5.3: The vertex invariant

Referring to the points in Figure 5.3, the *vertex invariant* is

$$\chi(v) = [A, B, C, D]. \quad (19)$$

A routine calculation, which we omit, shows that

$$\chi(v) = f_1 f_2, \quad (20)$$

where f_1 and f_2 are the invariants associated to the flags adjacent to v . Such a relation is not so surprising, because everything in sight just depends on the 5 points shown.

Lemma 5.3 *Let P be a PLC pentagram spiral. The quantity $Z^2(P)$ is a lower bound for the vertex invariants of P .*

Proof: This is immediate from Corollary 5.2 and from Equation 20. ♠

5.3 Uniform Bounds

One of the main goals in this chapter is to show that the invariant Z has compact level sets. In this section, we will consider a sequence $\{P(m)\}$ of pentagram spirals such that $Z(P(m))$ is independent of m . Our goal is to establish some uniform bounds for such spirals. We will normalize by projective transformations so that

$$P_1(m) = (0, 0), \quad P_2(m) = (1, 0), \quad P_3(m) = (1, 1), \quad P_4(m) = (0, 1) \quad (21)$$

for all m . Here $P_j(m)$ denotes the j th point of $P(m)$. We let $P_+(m)$ denote the union of all points $P_j(m)$ where $j \geq 1$. This is an inward spiraling half of $P(m)$.

Lemma 5.4 *There is some D such that $\|P_5(m) - P_4(m)\| < D$. Here D does not depend on m .*

Proof: It follows from Lemma 5.1 and from our normalization that $P_5(m)$ lies between the two lines $y = 0$ and $y = 1$, as shown in Figure 5.3.

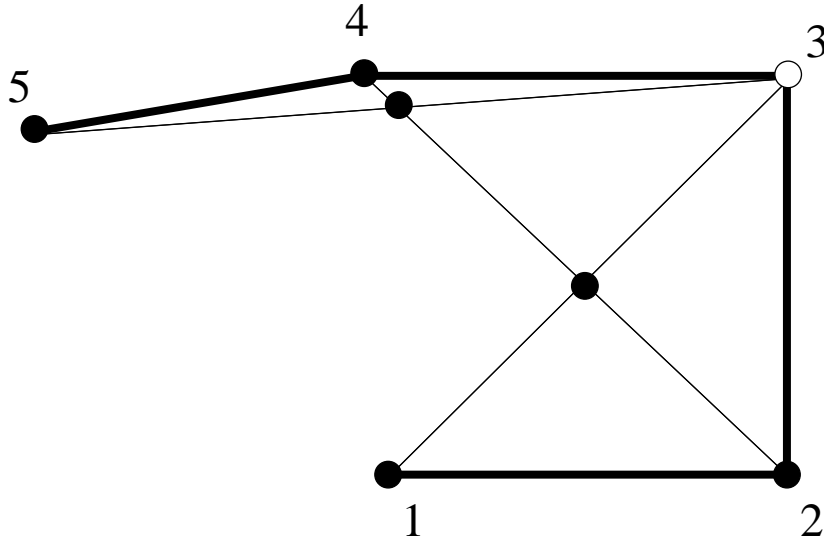


Figure 5.3: The points P_1, P_2, P_3, P_4, P_5 .

If $\|P_5(m) - P_4(m)\| \rightarrow \infty$ then the corner invariant $\chi(P_3)$ tends to 0 with m . This is impossible, by Lemma 5.3. ♠

Lemma 5.5 *There is some $d > 0$ such that $\|P_5(m) - P_4(m)\| > d$. Here d does not depend on m . Likewise, there is some $s > 0$ such that the line $P_4(m)P_5(m)$ has slope at least s . Here s is independent of m .*

Proof: These statements have the same proof as in Lemma 5.4. ♠

Lemma 5.6 *There is some compact subset $K \subset \mathbf{R}^2$ such that $P_+(m) \subset K$ for all m . In particular, there is some D such that $\|P_j(m) - P_{j+1}(m)\| < D$ for all m and all $j > 0$.*

Proof: The local convexity of $P(m)$ guarantees that $P_+(m)$ is contained in the quadrilateral $K(m)$ bounded by the lines $x = 1$ and $y = 0$ and $y = 1$ and $P_4(m)P_5(m)$. Given what we have established about $P_5(m)$, we have a uniform upper bound to the diameter of this quadrilateral. Hence there is a single compact K which contains $K(m)$ for all m . The second conclusion of the lemma is now immediate. ♠

Lemma 5.7 *Suppose that $j > 1$. Then $\|P_{j+1}(m) - P_j(m)\| > d$. Here d does not depend on m . Likewise, the segment $P_j(m)P_{j+1}(m)$ makes an exterior angle of at least $\theta > 0$ with $P_{j-1}(m)P_j(m)$. Again, θ does not depend on m .*

Proof: If this result fails, there is some smallest j where the problem goes wrong. This means that the points $P_{j-3}, P_{j-2}, P_{j-1}, P_j$ are spaced uniformly far apart independent of m . Moreover, there is a uniform lower bound to the exterior angles shown in Figure 5.4. But then the same argument as in the proof of Lemma 5.4, applied to $\chi(P_{j-1})$, gives a contradiction. ♠

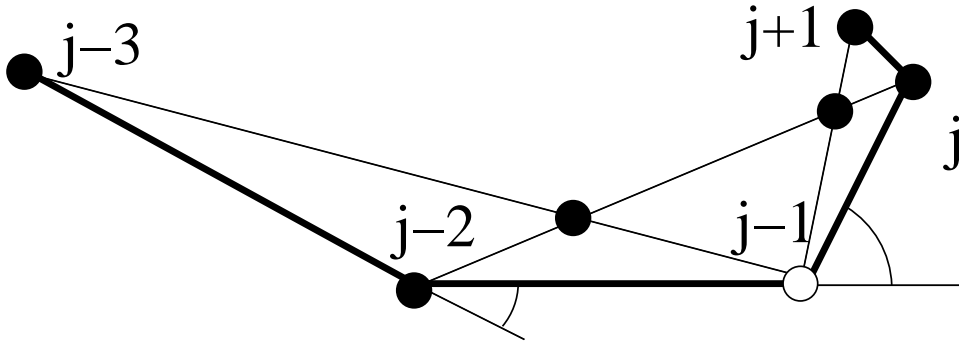


Figure 5.4: The points P_{j-3}, \dots, P_{j+1} .

Lemma 5.8 *Suppose that $j > 1$. The segment $P_j(m)P_{j+1}(m)$ makes an interior angle of at least $\theta > 0$ with $P_{j-1}(m)P_j(m)$. Here, θ does not depend on m .*

Proof: This is forced by the fact that every 5 consecutive points lie on a convex pentagon, together with the uniform lower bound on the side lengths. ♠

Corollary 5.9 *The sequence $\{P_+(m)\}$ converges, at least on a subsequence, to a strictly convex infinite polygonal path $P_+(\infty)$. Every 5 consecutive points of $P_+(\infty)$ are the vertices of a strictly convex pentagon.*

Proof: This follows immediately from the uniform bounds we have on all the lengths and angles, together with compactness. ♠

5.4 Compactness Proof

Now we put everything together and prove Theorem 1.2. As we mentioned above, it suffices to prove that the invariant $Z = Z(n, k)$ has compact level sets. Let $\{P(m)\}$ be as in the previous section. These pentagram spirals all have the same Z -invariant. Let $X_+(m)$ denote the portion of the triangulation associated to $P(m)$ which is contained in the seed

$$S'(m) = T_{n,k}^{4k+4}(S(m)). \quad (22)$$

We use the seed $S'(m)$ rather than $S(m)$ because our construction produces a union of triangles whose outermost portion is somewhat ragged.

We will show below that the sequence $\{X_+(m)\}$ converges to a triangulation which we will call $X_+(\infty)$. There are two kinds of edges in $X_+(m)$. The edges of the first kind are contained in $P(m)$ and its images under powers of the pentagram map. The union of these edges will converge to strictly locally convex paths in $X_+(\infty)$. The second kind of edge in $X_+(m)$ is a shortest diagonal of $P(m)$ or one of its images under powers of the pentagram map. These edges of the second kind will converge to the corresponding shortest diagonals of the strictly convex paths in $X_+(\infty)$ which we have just mentioned.

The convergence of triangulations implies that the sequence of seeds $\{S'(m)\}$ converges to a nontrivial seed $S'(\infty)$. Indeed, the convex polygon A' supporting $S'(\infty)$ is just the outer boundary of the tiling $X_+(\infty)$. Some of the edges of this outer boundary are edges of the first kind, and these determine the B' points marking k of the edges of A' . The convergence of seeds implies the compactness result.

For ease of exposition we suppose $k > 1$. The case $k = 1$ is similar and in fact easier. Each pentagram spiral $P(m)$ is part of a system of k pentagram spirals $P(m, j)$ for $j = 1, \dots, k$, which are permuted by the pentagram map.

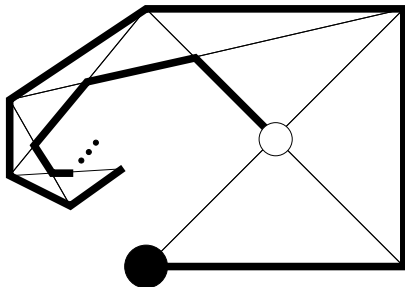


Figure 5.5: The image of $P_+(\infty)$ under the pentagram map.

Let $P_+(\infty, 1)$ be the limit guaranteed by Corollary 5.9. The pentagram map is well defined on $P_+(\infty, 1)$, starting from the first point onwards, as indicated by Figure 5.5. Let $P_+(\infty, 2)$ be the image of $P_+(\infty, 1)$ under the pentagram map. Evidently, $P_+(\infty, 2)$ is the limit of $\{P_+(m, 2)\}$, where $P_+(m, 2)$ is some forward-infinite portion of $P(m, 2)$. From our construction, we see that $P_+(\infty, 2)$ is a locally strictly convex infinite path. Moreover, every 5 consecutive points of $P_+(\infty, 2)$ are the vertices of a strictly convex pentagon. But now the pentagram map is defined on $P_+(\infty, 2)$, and we arrive at $P_+(\infty, 3)$, which is evidently the limit of a suitably defined sequence $\{P_+(m, 3)\}$.

We continue this way until we reach $P_+(\infty, k + 1)$. This is a proper sub-path of $P_+(\infty, 1)$, where roughly $n - k/2$ vertices have been chopped off the front. Let $X'_+(\infty)$ denote the union of the paths $P_+(\infty, j)$, for $j = 1, \dots, k$, together with all their shortest diagonals. The corresponding union $X'_+(m)$ contains the tiling $X_+(m)$.

By construction, $X'_+(m)$ converges to $X'_+(\infty)$. But then there is a subset $X_+(\infty)$ which is the limit of the slightly smaller $X_+(m)$. The outer boundary of $X_+(\infty)$ is the limit of the sequence $\{S'(m)\}$ of seeds. This convergence is what we had wanted to establish. The proof of Theorem 1.2 is done.

6 Geometry of the Tiling

6.1 Hilbert Diameter

Our goal in this chapter is to prove Theorems 1.3 and 1.4.

Let $K \subset \mathbf{RP}^2$ be a compact convex domain. Given 2 points $b, c \in K$, we have the Hilbert distance

$$d_K(b, c) = -\log[a, b, c, d] \quad (23)$$

where a and d are the two points where the line bc intersects ∂K , ordered as in Figure 6.1. This is a projectively natural metric on K . When K is a circle, d_K is the hyperbolic metric in the Klein model.

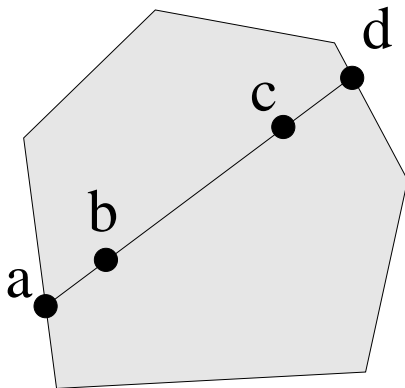


Figure 6.1: The Hilbert distance

Suppose that L is a compact set contained in the interior of K . We define the *Hilbert diameter* of L to be the diameter of L as measured in the Hilbert metric.

Lemma 6.1 *Suppose that $\{L_n\}$ is a sequence of compact convex subsets contained in the interior of K . Suppose that the Euclidean diameter of L_n converges to the Euclidean diameter of K . Then the Hilbert diameter of L_n converges to ∞ .*

Proof: Take a segment σ_m which connects two points on L_m which are maximally spaced apart. Call these points b_m and c_m . Let a_m and d_m be the points used in the definition of $d_K(a_m, b_m)$. By construction $\|a_m - b_m\|$ and $\|c_m - d_m\|$ converge to 0 whereas $\|b_m - c_m\|$ is uniformly bounded away from 0. In this situation $d_K(b_m, c_m) \rightarrow \infty$. ♠

6.2 Support of the Tiling

Now we turn to the proof of Theorem 1.3. We begin with a corollary of Lemma 6.1.

Corollary 6.2 *Suppose that $\{K_m\}$ is a nested family of compact convex subsets, with K_{m+1} contained in the interior of K_m for all $m \in \mathbf{Z}$. Suppose that there is some uniform constant C such that the Hilbert diameter of K_{m+1} with respect to K_m is less than C for all m . Then $\bigcap K_m$ is a single point.*

Proof: We just use the upper bound on diameter. Lemma 6.1 implies that the Euclidean diameter of K_{m+1} is at most λ times the Euclidean diameter of K_m , for some uniform $\lambda < 1$. ♠

Now we turn to the triangulation X associated to a pentagram spiral P . We think of X as a union of solid triangles.

Let (A_0, B_0) be the seed generating P . Define

$$(A_m, B_m) = T^{mn}(A_0, B_0). \quad (24)$$

Let K_m be the convex region bounded by the polygon A_m . By construction, K_{m+1} is contained in the interior of K_m .

By Theorem 1.2 and compactness, there is an upper bound C such that the Hilbert diameter of K_{m+1} with respect to K_m is less than C , independent of m . Here we are using the projective naturality of the Hilbert metric. The point is that we are just sampling a pre-compact subset of seeds in $\mathcal{C}(n, k)$. Corollary 6.2 now says that

$$\bigcap K_m \quad (25)$$

is a single point. But X contains $K_m - K_{m+1}$. Hence X contains all points of K_0 except for this one intersection point. This is what we wanted to prove.

Next we claim that X is a triangulation of $\mathbf{RP}^2 - L$, where L is a single line. This is equivalent to the statement that the ω limit set of P_- is a single line L . Here P_- is the outward portion of P .

As is well known, projective dualities conjugate the (suitably interpreted) pentagram map to its inverse. Thus, the ω -limit set of P_- is dual to the ω -limit set of P_+^* , the inward part of the dual pentagram spiral. We have already proved that the latter is a single point. Hence, the former is a single line.

This completes the proof of Theorem 1.3.

6.3 Winding of Pentagram Spirals

Let P be a pentagram spiral, with distinguished vertex P_1 . We translate the picture so that $P \subset \mathbf{R}^2$ and so that the origin is the limit point and P_1 is on the positive x -axis, as shown in Figure 6.2.

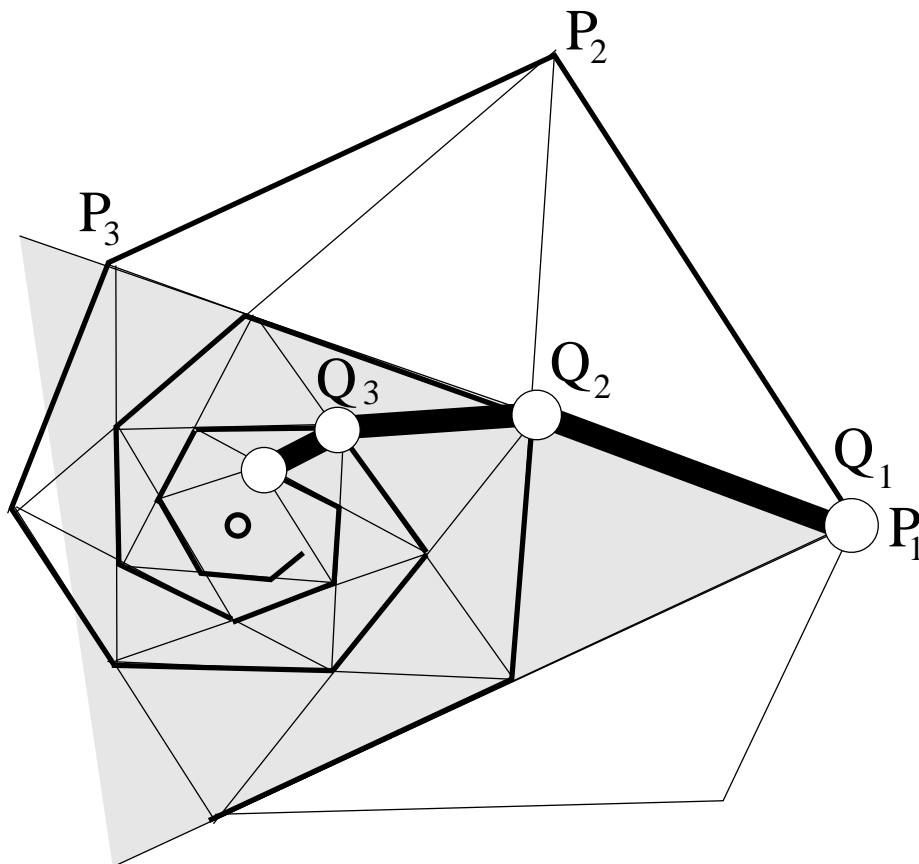


Figure 6.2: The spine

The vertex $Q_1 = P_1$ is the apex of a (shaded) cone C which contains the inward spiraling direction of P starting at P_3 . Hence C contains the limit point of P , namely the origin. The top edge of C leads to a point Q_2 lying in the upper half plane. The important point here is that $\arg(Q_2) > \arg(Q_1)$. We can repeat the same construction at Q_2 . There is a cone which contains the origin, and one of the edges of this cone leads to a point Q_3 such that $\arg(Q_3) > \arg(Q_2)$.

Let P_+ be the inward spiraling direction of P . Let Q_+ be the polygonal path connecting the points Q_1, Q_2, Q_3, \dots as shown in Figure 6.2. Both these paths converge to the origin in the forward direction. Since Q_+ contains infinitely many points and each such point lies on one of the finitely many spirals in the tiling, we see that some spiral contains infinitely many point of Q_+ . But, in fact, by inspecting the picture we see that whenever some point of Q_+ intersects a spiral, the next point of Q_+ intersects the next spiral. Thus P_+ and Q_+ intersect infinitely often.

Since the argument increases along both P_+ and along Q_+ , we see that the argument increases by more than 2π along P_+ between every two intersections with Q_+ . Hence, the argument along P_+ increases without bound. This proves Theorem 1.4.

Remark: The proof of Theorem 1.4 is really quite simple. The only way it relies on the previous material is that we would like to say that the pentagram spiral P really does have a single limit point.

7 Experiments and Discussion

7.1 Periodicity

With respect to specially chosen labeling schemes, the pentagram map is the identity on $\mathcal{C}(5)$ and has period 2 on $\mathcal{C}(6)$. See [Sch1]. Referring to the pentagram spirals, I discovered the following result computationally.

Theorem 7.1 *The following is true.*

- $T_{4,1}^2$ is the identity on $\mathcal{C}(4, 1)$.
- $T_{4,2}^2$ is the identity on $\mathcal{C}(4, 2)$.
- $T_{5,1}^8$ is the identity on $\mathcal{C}(5, 1)$.

Theorem 7.1 says that all the pentagram spirals of this kind are self-projective. Theorem 7.1 can be expressed in terms of seeds and the seed map, and so it only involves a finite number of points and lines. Thus, Theorem 7.1 can be established by a finite calculation, similar in spirit to what is done in [ST]. I have not yet made the rigorous calculations. Some of the results in [ST] have conceptual proofs, and I wonder if there are likewise conceptual proofs for the statements in Theorem 7.1

It seems discussing how I discovered this. My computer program allows the user to normalize the spirals so that the first 4 points are the vertices of the unit square. One can then watch an animation which shows the iteration of $T_{n,k}$. I put in an option which allows the user to choose a smallish integer q and watch the movie showing $T_{n,k}^q$.

For instance, for the parameter $(n, k) = (4, 3)$ the choice $q = 18$ makes for a nice movie. The point is that, for a random choice of pentagram spiral of type $(4, 3)$, the 18th power of the shift map is fairly close to the identity, so an animation of the map looks somewhat like a flow to the naked eye. As another example, for $(n, k) = (6, 2)$ the choice $q = 54$ often produces a nice movie. I have found a few of these values experimentally, but not many. The reader can see all of this in action on my program.

For the combinatorial type $(4, 1)$, I noticed that the image on the computer screen, for $q = 1$ just flickered back and forth. When I put in $q = 2$ the image was just stationary. Likewise, for the combinatorial type $(4, 2)$, the choice $q = 2$ “froze the movie” and for the combinatorial type $(5, 1)$ the choice $q = 8$ “froze the movie”. I would say that this is overwhelming experimental support for Theorem 7.1.

7.2 Asymptotic Shape

We can combine Theorem 7.1 with some of our other results to get more information about the special cases $(4, 1)$, $(4, 2)$.

Theorem 7.2 *Any PLC pentagram spiral of type $(4, 1)$ or $(4, 2)$ is projectively equivalent to a self-similar polygonal path.*

Proof: We can normalize by a projective transformation so that our pentagram spirals lie in the plane and have the origin as their limit point. If P is a pentagram spiral as in Theorem 7.1, then there is a projective transformation S so that $S(P) = P$. Necessarily S preserves the ω -limit set of P . Hence S preserves the line at infinity and fixes the origin. That is, S is a linear transformation.

Now, the action of S shifts the indices of P by 2, or 8 depending on the case. In the cases $(4, 1)$ and $(4, 2)$ one can argue that the path made from the short diagonals of P again winds infinitely often around the origin. But this means that the orbits of S wind infinitely often around the origin. But then S is conjugate to a similarity. So, in the cases $(4, 1)$ and $(4, 2)$, there is a canonical normalization of the pentagram spirals so that they are self-similar. ♠

The case $(4, 1)$ yields a 1-parameter family of distinct shapes and the case $(4, 2)$ yields a 2 parameter family of shapes. The argument above breaks down in the case $(5, 1)$, but experimentally the result seems to be true.

To describe some experimental results along these lines, we need to introduce some terminology. Let Γ be an infinite polygonal path which limits on the origin in one direction and exits every compact set of the plane in the other direction. We call Γ *quasi-logarithmic* (or QL for short) if there is some nontrivial homothety D such that the family of curves $\{D^n(\Gamma)\}$ is precompact in the Hausdorff topology on shapes. To say that Γ is QL is to say that Γ is only boundedly far from being invariant under a homothety. For instance, a logarithmic spiral is quasi-logarithmic.

I mentioned above that my computer program normalizes pentagram spirals so that 4 distinguished vertices are the vertices of a unit square. I also programmed things so that different normalizations are possible. For instance, one can normalize by a homothety so that the distinguished vertex is a point of the unit circle. If a particular pentagram spiral is QL, then the

movie shown with this alternate normalization would “go on forever” keeping more or less the same shape.

It seems that for most choices of n and k , the pentagram spirals of type (n, k) are QL. For instance, when $n \leq 6$, only the case $(6, 1)$ seems to produce pentagram spirals which are not QL. In general, it seems that the larger values of k produces pentagram spirals which are more likely to be QL. I would need to do more experiments before making a definitive conjecture on this, so let me just pose this as a question:

Question: Are there values (n, k) such that every PLC pentagram spiral is QL? If so, which values?

7.3 Logarithmic Pentagram Spirals

For each choice of (n, k) there is a self-similar pentagram spiral P which I call the *logarithmic pentagram spiral* (or LPS for short.) The vertices of P lie in a logarithmic spiral and the edges of P are inscribed in a rotated copy of the logarithmic spiral. The pentagram map carries P to a rotated copy of P .

The LPS can be normalized so that it has vertices $\{z^n \mid n \in \mathbf{Z}\}$, where

$$|z| < 1, \quad \frac{2\pi}{n+k} < \arg(z) < \frac{2\pi}{n}, \quad (z + \bar{z})^k = z^{n+k}(1 + \bar{z})^k. \quad (26)$$

These equations come from the observation that the intersection of the line through 1 and z^2 with the line through z and z^3 is

$$w = \frac{z(z + \bar{z})}{1 + \bar{z}},$$

and that the combinatorics of the spiral dictate that $w^k = z^{n+2k}$. I had a lot of trouble solving Equation 26 on Mathematica, but I will describe a different way to draw very close approximations to the LPS.

Say that the seed $P = (A, B)$ is *normalized* if

$$A_1 = (0, 0), \quad A_2 = (1, 0), \quad A_3 = (1, 1), \quad A_4 = (0, 1). \quad (27)$$

That is, the first 4 vertices of P are the vertices of the unit square. Each point of $\mathcal{C}(n, k)$ has a unique normalized representative. A normalized representative consists of a convex n -gon and k additional points. The locations

of these points can be described by the quantities

$$d_i = \frac{\|A_i - B_i\|}{\|A_i - A_{i+1}\|} \in (0, 1), \quad i = (n - k + 1), \dots, n. \quad (28)$$

The point A_{n+1} is interpreted as A_1 .

Given some point $P = (A, B) \in \mathcal{C}(n, k)$ and some integer j , we define $P^j = (A^j, B^j)$ as the normalized version of $T_{n,k}^j(P)$. Given some integer m , define $\Theta_m(P) = (A', B')$, where A' is the pointwise average of the polygons A^0, \dots, A^{m-1} and the number d'_j is the average of the corresponding numbers for P^0, \dots, P^{m-1} . In practice, Θ_m seems to act as a kind of contraction mapping on $\mathcal{C}(n, k)$, and the fixed point is the logarithmic pentagram spiral.

So, one can choose some smallish m and iterate Θ_m several times. This produces a point in $\mathcal{C}(n, k)$ very close to the point representing the logarithmic pentagram spiral. Given a point in $\mathcal{C}(n, k)$ representing the logarithmic pentagram spiral, one can then apply projective transformations to find better normalizations. The cheapest way to do this is just to apply $T_{n,k}$ many times and then dilate the picture. This method produced the picture shown in Figure 7.1.

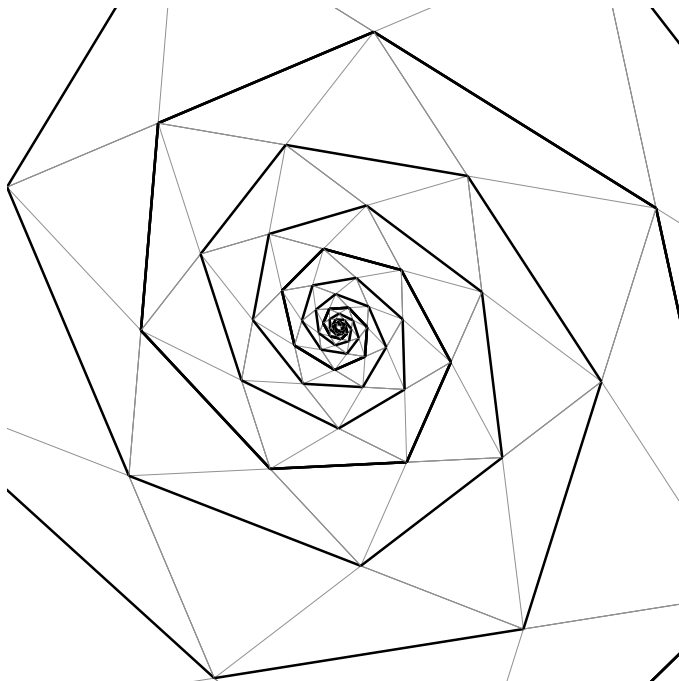


Figure 7.1: Approximation to the LPS of type (5, 3).

The logarithmic pentagram spiral is a natural origin for the space $\mathcal{C}(n, k)$ just as the projective class of the regular n -gon is a natural origin for the space $\mathcal{C}(n)$. Computer experiments suggest the following conjecture

Conjecture 7.3 *For any (n, k) , the invariant Z is uniquely maximized, and has a unique critical point, at the point representating the logarithmic pentagram spiral.*

There is an analogous conjecture for the space $\mathcal{C}(n)$. Corollary 1.2 in my paper [Sch4] proves that (the analogue of) Z is maximized at the regular polygons when restricted to the subspace of polygons which are inscribed in circles.

7.4 Twisted Pentagram Spirals

The notion of a twisted polygon has been very useful in the study of the ordinary pentagram map. See [Sch3], [OST1], and [OST2]. A *twisted n -gon* is a map $\phi : \mathbf{Z} \rightarrow \mathbf{RP}^2$ which intertwines translation by n with a projective transformation M . That is,

$$\phi \circ \mu = M \circ \phi(k), \tag{29}$$

Here μ is translation by n . That is, $\mu(k) = k + n$. The transformation M is the *monodromy* of the twisted polygon.

The pentagram map acts on twisted n -gons and again commutes with projective transformations. One can define $2n$ flag invariants of a twisted n -gon just as for an ordinary ones. The flag invariants of twisted n -gon and its iterates under the pentagram map naturally give rise to a labeling of \mathbf{T} , as in §4.2. This labeling is an element of $\mathcal{T}(n, 0)$.

Now we want to do the same kind of thing for pentagram spirals. First of all, we fix a *model* tiling generated by a particular element of $\mathcal{C}(n, k)$, say the logarithmic pentagram spiral. (The model is just used for combinatorial purposes.) Next, we create a locally identical tiling of the universal cover \widetilde{X} of $\mathbf{R}^2 - (0, 0)$. That is, we simply pull back the tiling to \widetilde{X} . Let \widetilde{T} denote the tiling of the universal cover.

The space \widetilde{X} is homeomorphic to the plane, but it has an exotic projective structure on it. A straight line in this universal cover is something which projects to a straight line. There is a \mathbf{Z} -action on \widetilde{X} , namely the deck

group. The deck group acts so as to carry lines to lines. Let μ be a generator of the deck group. We have $\mu(\tilde{T}) = \tilde{T}$.

A *twisted pentagram spiral* is an adapted map ϕ satisfying Equation 29 with respect to the deck group generator μ . By *adapted map* I mean that ϕ is a homeomorphism when restricted to each (solid) triangle of \tilde{T} and that ϕ carries each line segment in the 1-skeleton of \tilde{T} to a straight line segment in \mathbf{RP}^2 . Note that some of these line segments consist of 3 consecutive edges of triangles.

An ordinary pentagram spiral is simply a twisted pentagram spiral having monodromy the identity. Moreover, the above definition reduces to the usual definition in the case of closed polygons. It is merely the original definition rephrased in terms of the triangulation produced by the pentagram map.

Some readers might not like the above geometric definition of a twisted pentagram spiral, so let me describe things algebraically. A projective equivalence class of A twisted pentagram spiral is nothing more than an element of $\mathcal{T}(n, k)$. Starting with an element of $\mathcal{T}(n, k)$, one can start building a network of line segments in the projective plane, such that the corresponding flag invariants give the labels of $\mathcal{T}(n, k)$. As one develops the picture going “all the way around” the cylinder $\mathbf{R}^2/V_{n,k}$, one might observe that the configuration in the projective plane does not close up. The failure of the picture to close up is encoded in the monodromy.

7.5 Integrability

Computer experiments suggest the following conjecture.

Conjecture 7.4 *The map $T_{n,k}$ acting on $\mathcal{C}(n, k)$ is a discrete totally integrable system.*

What I mean is that $\mathcal{C}(n, k)$ should have a singular foliation by tori, each equipped with a flat structure, such that each orbit of $T_{n,k}$ is contained in a finite union of tori. Moreover, the restriction of a suitable power of $T_{n,k}$ to each torus is a translation relative to the canonical flat structure. Such a structure would arise if $\mathcal{C}(n, k)$ had an invariant Poisson structure and sufficiently many commuting invariant functions. This how the torus foliation arises in [OST1] and [OST2] for the pentagram map.

I will describe, to some extent, the computer experiments which lead to this conjecture. The interested reader can do the experiments themselves using my program.

Let T be a PLC pentagram spiral, and let $c(T)$ denote the limit point of the inward spiraling direction of T . If we normalize T so that the first 4 vertices are the vertices of the unit square Q , then the point $c(T) \in \mathbf{R}^2$ is a canonical point associated to T . Assuming that T is a pentagram spiral of type (n, k) , we define

$$c_m = c(T_{n,k}^m(T)). \quad (30)$$

That is, c_m is the limit point of the m th iterate of T under the shift map. My computer program allows the reader to view the sequence $\{c_m\}$.

For instance, the points $\{c_m\}$ seem to lie on a union of two (generically) smooth curve when $(n, k) = (5, 2)$. When we consider the thinner sequence $\{c_{18n}\}$ in this case, we see points appearing in order on a smooth curve. In other words, the movie we produce for the choices $(n, k) = (5, 2)$ and $q = 18$ shows the limit point gently rotating around a smooth curve. Again, we encourage the reader to download the program, so that he or she can see this in action.

The space $\mathcal{C}(5, 2)$ is 4-dimensional. The experiments above suggest that $\mathcal{C}(5, 2)$ is foliated by invariant loops and so that $R_{5,2}^2$ preserves each loop in the foliation and acts there as a (typically) irrational rotation. As is the case with the pentagram map, one would describe this situation as “mildly hyperintegrable”: The completely integrable situation would predict invariant 2-tori.

As n and k increase, it is harder to see that the sequence $\{c_m\}$ is the projection of a sequence of curves lying on a finite union of tori. However, for smallish values of m and k , one still gets a sense that this is the case.

7.6 Monodromy Invariants

The first step to proving the integrability conjecture is to find the integrals (i.e. invariants) of the map $T_{n,k}$. For the pentagram map, these invariants by now have many constructions. I will describe the original way I thought of them. Let M be the monodromy of a twisted N -gon. If we replace the twisted N -gon by a projectively equivalent one, the monodromy M is replaced by a conjugate. However, the two quantities

$$\frac{\mathrm{Tr}(M)}{\det^{1/3}(M)}, \quad \frac{\mathrm{Tr}(M^*)}{\det^{1/3}(M^*)}. \quad (31)$$

only depend on the projective equivalence class. In Equation 31 we think of M and M^* as matrices representing the action of the monodromy on the

projective plane and on the dual projective plane respectively.

The quantities in Equation 31 are rational functions of the flag invariants. There is a certain natural weighting of the monomials in these rational functions, and the homogeneous parts with respect to this weighting are the monodromy invariants. See [Sch3], [OST1] and [OST2] for details about this.

The special weighting can be described as follows. If we take any element of $\mathcal{T}(n, k)$ we can multiply all the forward slanting edges by s and all the backward slanting edges by $1/s$. This produces a new element of $\mathcal{T}(n, k)$. All the compatibility equations hold for the new equations. Every paper which has discussed the integrability of the pentagram map (and its generalizations) uses this scaling in a crucial way.

Now, the monodromy of a pentagram spiral can be computed using a path which only encounters finitely many edges of the tiling \tilde{T} . This, it would seem that the quantities in Equation 31 would also be rational functions in finitely many of the flag invariants. The scaling mentioned above works just fine here. So, the weighted homogeneous parts ought to be invariants of the map $T_{n,k}$ on the larger space $\mathcal{T}(n, k)$, which we might as well interpret as the space of twisted pentagram spirals of type (n, k) . Restricting these invariants to the subset $\mathcal{C}(n, k)$ we would get invariants for the shift map $T_{n,k}$.

I tried to compute the monodromy invariants for the very modest case $(n, k) = (4, 1)$ and I arrived at depressingly complicated expressions. This makes me somewhat pessimistic that one could arrive at crisp formulas like Equation 31 in the general case. It seems to me that the calculation will have to wait either for a more determined experimenter or for a better coordinate system.

My guess is that the Poisson bracket of [OST1] and [OST2] will generalize to the case of pentagram spirals as well. But I will leave this discussion for a later paper.

8 References

- [FM] V. Fock, A. Marshakov, *Integrable systems, clusters, dimers and loop groups*, preprint, 2013
- [GK] A. B. Goncharov and R. Kenyon, *Dimers and Cluster Integrable Systems*, preprint, arXiv 1107.5588, 2011.
- [GSTV] M. Gekhtman, M. Shapiro, S. Tabachnikov, A. Vainshtein, *Higher pentagram maps, weighted directed networks, and cluster dynamics*, Electron. Res. Announc. Math. Sci. **19** 21012, 1–17
- [Gli] M. Glick, *The pentagram map and Y-patterns*, Adv. Math. **227**, 2012, 1019–1045.
- [Gli1] M. Glick, *The pentagram map and Y-patterns*, 23rd Int. Conf. on Formal Power Series and Alg. Combinatorics (FPSAC 2011), 399–410.
- [KDif], R. Kedem and P. DiFrancesco, *T-Systems with boundaries from network solutions*, preprint, arXiv 1208.4333, 2012
- [KS] B. Khesin, F. Soloviev *Integrability of higher pentagram maps*, Mathem. Annalen. (to appear) 2013
- [MB1] G. Mari Beffa, *On Generalizations of the Pentagram Map: Discretizations of AGD Flows*, arXiv:1303.5047, 2013
- [MB2] G. Mari Beffa, *On integrable generalizations of the pentagram map* arXiv:1303.4295, 2013
- [Mot] Th. Motzkin, *The pentagon in the projective plane, with a comment on Napiers rule*, Bull. Amer. Math. Soc. **52**, 1945, 985–989.
- [OST] V. Ovsienko, R. Schwartz, S. Tabachnikov, *Quasiperiodic motion for the pentagram map*, Electron. Res. Announc. Math. Sci. **16** ,2009, 1–8.
- [OST1] V. Ovsienko, R. Schwartz, S. Tabachnikov, *The pentagram map: A discrete integrable system*, Comm. Math. Phys. **299**, 2010, 409–446.

[**OST2**] V. Ovsienko, R. Schwartz, S. Tabachnikov, *Liouville-Arnold integrability of the pentagram map on closed polygons*, to appear in Duke Math. J.

[**Sch1**] R. Schwartz, *The pentagram map*, Experiment. Math. **1**, 1992, 71–81.

[**Sch2**] R. Schwartz, *The pentagram map is recurrent*, Experiment. Math. **10**, 2001, 519–528.

[**Sch3**] R. Schwartz, *Discrete monodromy, pentagrams, and the method of condensation*, J. of Fixed Point Theory and Appl. **3**, 2008, 379–409.

[**Sch4**] R. Schwartz, *A Conformal Averaging Process on the Circle* Geom. Dedicata., 117.1, 2006.

[**Sol**] F. Soloviev *Integrability of the Pentagram Map*, to appear in Duke Math J.

[**ST**] R. Schwartz, S. Tabachnikov, *Elementary surprises in projective geometry*, Math. Intelligencer **32**, 2010, 31–34.